1-1-2016

Regulators Of Ins-6, A Major Node Of The Insulin-Like Peptide Network For Developmental Plasticity

Lisa Li
Wayne State University,

REGULATORS OF *INS-6*, A MAJOR NODE OF THE INSULIN-LIKE PEPTIDE NETWORK FOR DEVELOPMENTAL PLASTICITY

by

LISA LI

THESIS

Submitted to the Graduate School

of Wayne State University,

Detroit, Michigan

in partial fulfillment of the requirements

for the degree of

MASTER OF SCIENCE

2016

MAJOR: BIOLOGICAL SCIENCES

Approved By:

_____

Advisor Date

ACKNOWLEDGEMENTS

First and foremost, many acknowledgements go to my advisor, Joy Alcedo. I feel extreme gratitude she was my mentor, for the patience she has always displayed, all the discussions, her encouragement, and for seeing my potential. I would be remiss if I did not also thank Rashmi Chandra. Her work and great observations gave rise to my project. This was a collective effort and I am indebted to her for her guidance. I would also like to thank our collaborators: Yun Zhang at Harvard University, and Queelim Ch'ng at King's College. Great appreciation also goes to my committee members, Karen Beningo and David Njus, for their support and guidance throughout my time in the program. Also, thanks go to Krystyn Purvis for always helping me with any teaching problems.

Many thanks go to former and current lab members. Particular acknowledgments go to Zahabiya Husain for technical support with screening, hybridization of samples, and crosses, Deniz Sifoglu for help with bioinformatic analysis, and Tiffany Burris for help with the screen. To Erika Allen, Shashwat Mishra, Kelsey Marbach, Sean Shepard, Aria Ganz-Waple, Ian Clark, Serina Beydoun and others: I treasure the laughs we've shared, lunches, drinks, and friendships. Special friends in the department include Wesley Colangelo, who has a sixth sense and knows exactly when I need coffee.

Last, but not least, I would like to thank my family. I thank my older brother Ming for always setting the bar high and being a great role model for me. And to my parents, I would like to just simply say: without your love and support, I don't know where I would be. Thank you for everything you have done for me and will continue to do.

TABLE OF CONTENTS

LIST OF TABLES

LIST OF FIGURES

1. INTRODUCTION

The environment is a major influence in the development of any living organism. External factors, such as food abundance, temperature, water levels, and the presence of predators versus prey, are just a few examples of cues that could affect an animal's survival in nature. The worm *Caenorhabditis elegans* is no different. It senses and processes environmental information and adjusts its physiology accordingly to enhance its survival. Indeed, *C. elegans* has adapted an alternative developmental program, known as dauer arrest, which allows it to alter its physiology and withstand harsh conditions much better than its non-arrested forms.

1.1 The Life Cycle of *C. elegans*

Under ideal conditions, like an abundance of food, ambient temperatures of ~23.5°C, and low population density, *C. elegans* will first hatch from an egg into the first larval stage known as L1, which will then continue to develop into the next larval stages of L2 to L4 (Byerly et al., 1976)[Figure 1.1]. At the end of the L4 stage, the worm will molt into a reproductive adult. The hermaphroditic *C. elegans* adult starts to produce oocytes that are fertilized by the sperm it produces during the L4 stage (Kimble and Hirsh, 1979). The fertilized eggs are stored in the worm uterus and laid through the vulva once the embryos are undergoing gastrulation (Bucher and Seydoux, 1995). On average, a wild-type worm will lay a brood size of approximately 300 eggs over a span of five to eight days at 20^{o}C (Byerly et al., 1976; Hirsh and Vanderslice, 1976).

However, when an L1 larva senses harsh conditions, like food scarcity, high temperatures, and/or high population density, it can decide to undergo an alternative developmental process called dauer arrest (Golden and Riddle, 1984). *C. elegans* senses population density through a pheromone mixture of glycosides that the animal secretes throughout its lifetime (Butcher et al., 2007; Jeong et al., 2005). Hence, high concentrations of this pheromone mixture, also known as dauer pheromone, will also signal an L1 that there is low food in the environment.

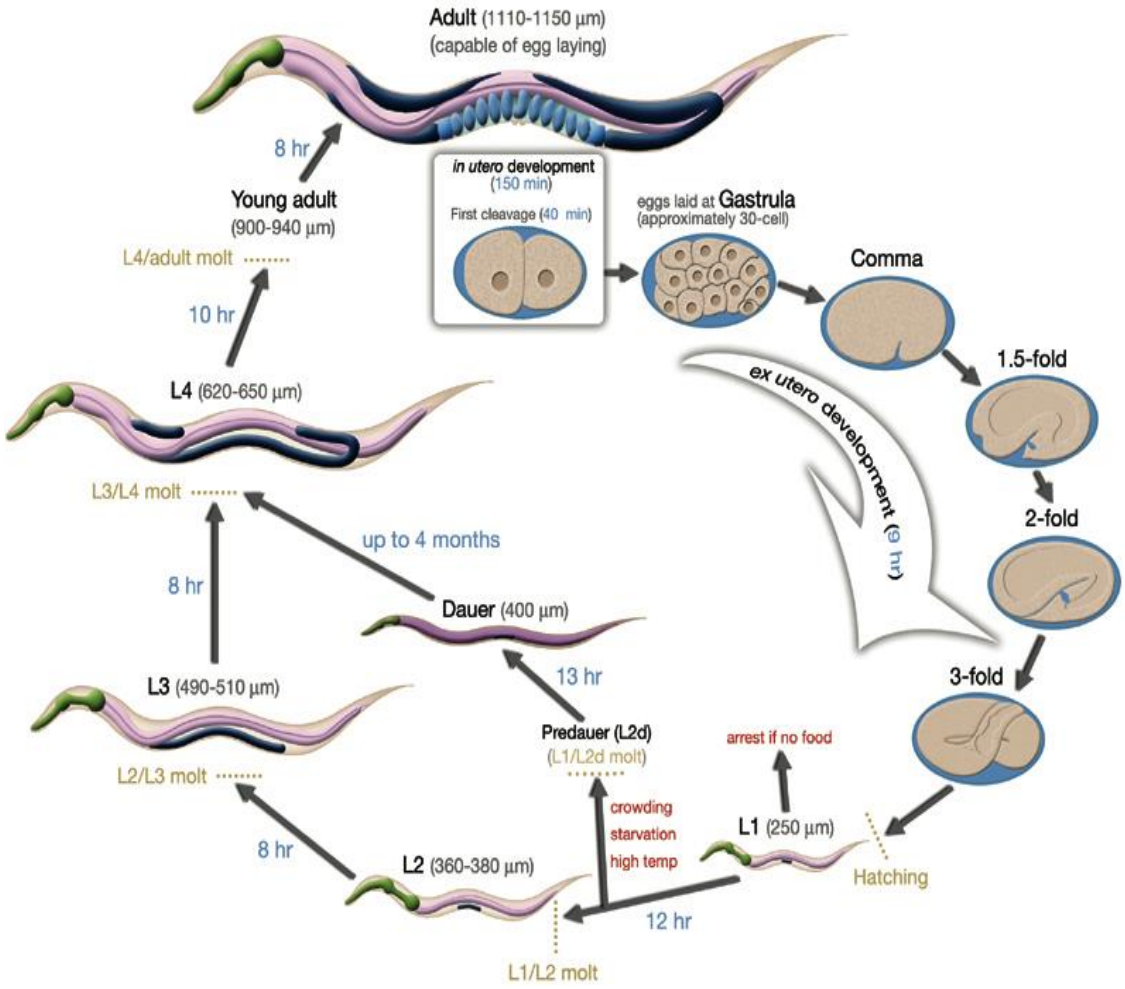

Figure 1.1 – The life cycle of C. elegans
By the time a hermaphrodite lays an embryo, it has already entered gastrulation. Several stages of ex utero development later, the worm hatches as a first-stage larva (L1). During this time, the L1 senses the environment and can make a decision. At the mid-L1 stage, the animal can continue on with the reproductive developmental program and mature as a second-stage larva (L2), which will then be followed by the third (L3) and fourth (L4) larval stages and ultimately reproductive adulthood. However, if an L1 senses harsh conditions, such as overcrowding (as indicated by high levels of dauer pheromone in the environment), starvation, or high temperatures, it will develop into a predauer (L2d). If harsh conditions persist, the worm will arrest as a dauer, a hardier alternative to the L3 stage and is long-lived and more stress resistant. Once food supply is replenished and conditions become more ideal, the dauer can exit to become a post-dauer L4 within 10 hours, where it can now resume reproductive development. (Figure taken from Hall and Altun, 2008).

A worm entering dauer developmental arrest will first remodel itself to become a pre-dauer or L2d (Riddle and Albert, 1997) [Figure 1.2]. Pre-dauers are not yet fully committed to

developing as a dauer. If environmental conditions reverse themselves, *C. elegans* can still molt from an L2d to an L3 and continue through reproductive development (Golden and Riddle, 1984; Riddle and Albert, 1997). However, if harsh conditions persist, the L2d worm will undergo further remodeling and molt into an arrested dauer (Riddle and Albert, 1997). This dauer, which has a different physiology, is the developmentally arrested alternative to a well-fed L3 larva (Cassada and Russell, 1975; Riddle et al, 1981). While in this diapause state, the dauer is now much more capable of weathering and surviving the harsh environment, compared to its L3 counterpart (Cassada and Russell, 1975; Golden and Riddle, 1982; Riddle et al., 1981)

1.2 Dauer Physiology

There are several physiological differences between L3s and dauers (Cassada and Russell, 1975; Riddle et al., 1981; Vowels and Thomas, 1992; Wadsworth and Riddle, 1989). Dauers stop feeding, since their buccal cavities become plugged with a cuticular block (Riddle et al., 1981) and their pharynges become constricted (Vowels and Thomas, 1992). Unlike other stages, dauers also develop a much thicker cuticle, which help them withstand toxic compounds, such as detergents (Cassada and Russell, 1975). The basal locomotion of dauers are also markedly reduced compared to L3s. However, the dauer cuticle has raised longitudinal ridges, known as alae, which are speculated to help dauers escape predation much faster than the other stages (Golden and Riddle, 1984). This is consistent with increased number of alae found in dauers compared to the number of alae found in other stages (Golden and Riddle, 1984).

Dauers also become very thin compared to their L3 counterpart, with a length-width ratio of about 30:1 (Hall and Altun, 2008). As the dauers become thinner, the lumens of the intestine and pharynx also shrink. Since dauers are developmentally arrested animals, they have a gonad like that of an L2, despite being the developmentally arrested alternative to the L3 larva. When favorable conditions are restored, dauers exit arrest and molt to the last larval stage (L4), from which they can resume reproductive development (Riddle and Albert, 1997).

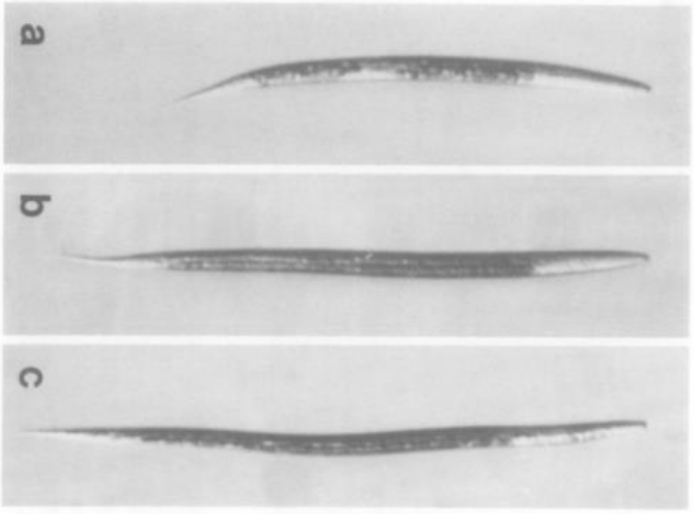

Figure 1.2 – Photomicrographs of select developmental stages. Panel (a) shows an L2 larva grown under ideal conditions. Panel (b) shows an L2d, or pre-dauer, formed after exposure to dauer pheromone. Panel (c) shows a dauer 12 hours after radial shrinkage, a result of exposure to dauer pheromone. (Taken from Golden and Riddle, 1984)

1.3 Sensory neurons influence the dauer pathway

C. elegans senses a variety of environmental cues, such as food type, food quantity, population density, and the presence of pathogenic and/or volatile compounds, which can then influence its homeostasis. The processing of environmental information can lead sensory neurons to secrete long-range signals that act as hormones or various small-molecule and/or peptide neurotransmitters that target neighboring neuronal or non-neuronal cells.

The *C. elegans* head has a pair of major sensory organs, known as amphids, which are bilaterally symmetric and can sense volatile, water-soluble and noxious cues (Bargmann and Horvitz, 1991a; Ward et al., 1975). Each amphid has twelve sensory neurons and eleven are chemosensory in nature: ADF, ADL, ASE, ASG, ASH, ASI, ASJ, ASK, AWA, AWB, and AWC. Each neuron has a dendrite that extends from the cell body to the amphid opening at the tip of the worm's head and each dendritic ending has a cilium or cilia that are fully or partly surrounded by a sheath cell (White et al., 1986). The cilia of neurons that sense volatile cues are not directly exposed to the environment and are thus olfactory in nature, whereas the cilia of neurons that sense water-soluble cues are directly exposed to the environment and act in gustation (Bargmann et al., 1993) [Figure 1.3]. The cilia of olfactory neurons have a wing-shaped structure (AWA, AWB, and AWC), whereas the cilia of gustatory neurons can have a single rod-like structure (ASE, ASG, ASH, ASI, ASJ, and ASK) or a double rod-like structure

(ADF and ADL) (White et al., 1986). The amphid neurons also have axons that extend to the nerve ring, where they bundle or fasciculate together with other neurons, making synaptic connections with each other (Ware et al, 1975). The nerve ring serves as the primitive brain of the worm [Figure 1.4].

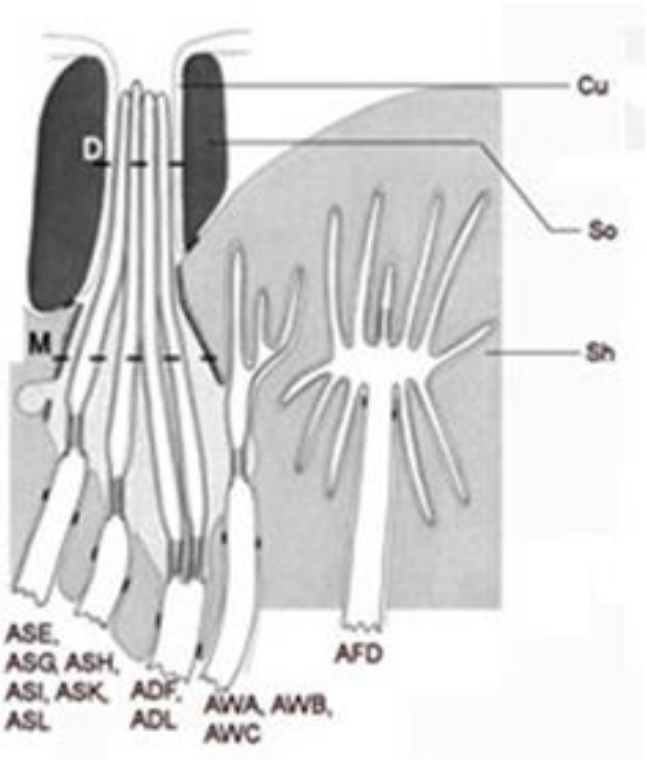

Figure 1.3 – Dendritic morphology of the amphid sensory neurons
Shown here are the ciliated cell bodies of the amphid neurons and the position of their dendrites. The glial socket cell (So) forms the amphid pore, which allows cilia to be directly exposed to the environment. Some cilia are not directly exposed to the environment and extend, instead, to sheath cells (Sh), where they sense cues that enter via diffusion. Cu, cuticle; So, socket cell; Sh, sheath cell (Taken from Inglis, P.N. *et al*, 2007, WormBook).

A small subset of the amphid chemosensory neurons has been shown to regulate dauer entry and exit (Bargmann and Horvitz, 1991a; Schackwitz et al., 1996). Through cell ablation studies, it was shown that the sensory neurons ASI and ADF, and ASG to a minor degree, inhibit dauer entry, as destruction of these neurons led to the formation of dauers (Bargmann and Horvitz, 1991b; Schackwitz et al., 1996), whereas ASK promotes dauer entry (Kim et al., 2009; Schackwitz et al., 1996). In contrast, ASJ has two opposing functions: it can induce dauer entry in L1 when conditions are harsh (Schackwitz et al., 1996) and promote dauer exit when environmental conditions improve (Bargmann and Horvitz, 1991) [Figure 1.4]. Hence, the neuronal subset that regulates dauer entry is not exactly the same as the subset that regulates dauer exit.

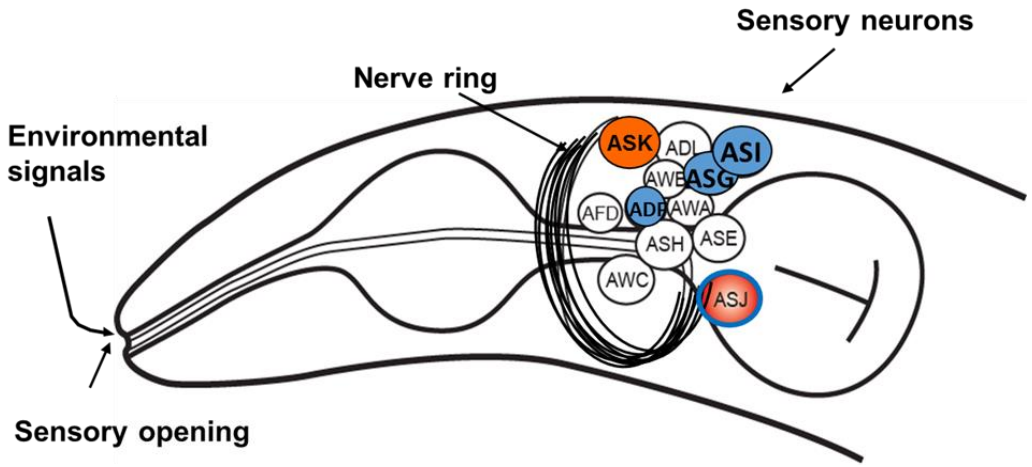

Figure 1.4 – Sensory neurons influence the dauer program
Shown here are sensory neurons located in the head of the worm. Axons of these neurons bundle together to form a ring-like structure known as the nerve ring, which acts as the primitive brain of the worm. These neurons also have dendrites that extend to the tip of the head to sensory openings, which allows them to sense various environmental cues. Neurons in blue (ADF, ASG, and ASI) inhibit dauer entry. ASK (indicated in red) promotes dauer entry, whereas ASJ, indicated in red with a blue line, plays a dual role in promoting dauer entry and promoting dauer exit.

1.4 The *daf-2* pathway is involved in dauer development

The DAF-2 pathway is also known as the insulin signaling pathway in *C. elegans*, as it is a hormone receptor that is similar to the human insulin receptor and IGF-1 receptor (Kimura et al., 1997). The binding of an agonistic ligand to DAF-2, a receptor tyrosine kinase, leads to the dimerization and autophosphorylation of the receptor monomers, which in turn activates a conserved signaling cascade [Figure 1.5]: from the activation of the AGE-1/phosphoinosotide-3 (PI3) kinase to the phosphorylation of PDK-1 and of the phospholipid PIP2 and to the subsequent activation of AKT (Kimura et al., 1997; Morris et al., 1996; Paradis et al., 1999; Paradis and Ruvkun, 1998). The downstream effects of AKT lead to phosphorylation of the FOXO transcription factor DAF-16, which would then be sequestered in the cytoplasm (Hertweck et al., 2004; Lee et al., 2001; Lin et al., 1997; Lin et al., 2001; Ogg et al., 1997). Therefore, DAF-2 and its agonists negatively regulate the activity of DAF-16/FOXO. On the

other hand, antagonistic DAF-2 ligands do not activate the signaling cascade that leads to phosphorylation of DAF-16, which prevents its sequestration in the cytoplasm and allows its translocation into the nucleus to regulate the expression of various target genes [Figure 1.5].

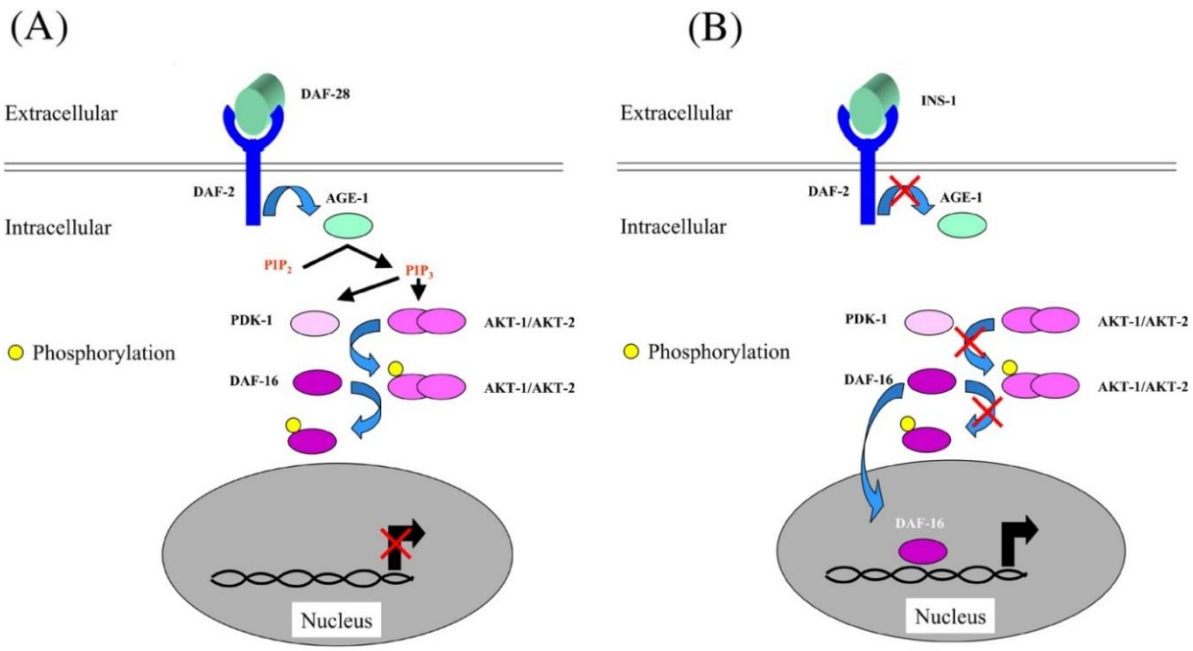

Figure 1.5 – The DAF-2 pathway in *C. elegans.*
(A) An agonist, such as the insulin-like peptide DAF-28, binds to the DAF-2 receptor tyrosine kinase, leading to the activation of a conserved signaling cascade. This signaling cascade results in the phosphorylation of DAF-16, sequestering it in the cytoplasm and negatively regulating its activity. (B) An antagonist, such as INS-1, binds to the DAF-2 receptor tyrosine kinase and does not result in activation of a signaling cascade. DAF-16 does not become phosphorylated and is able to enter the nucleus (Taken from Ewbank, 2006, Wormbook).

The DAF-2 pathway is known to be involved in regulating adult longevity. Mutations in *daf-2* result in adults that can live twice as long as their wild-type counterparts (Kenyon et al., 1993; Larsen et al., 1995). DAF-2 signaling also promotes larval reproductive growth, and downregulation of DAF-2 leads to dauer arrest (Kimura et al., 1997; Malone and Thomas, 1994; Riddle et al., 1981). The stronger the downregulation, the more constitutive is the induced dauer arrest, *i.e.*, the mutants do not exit arrest; on the other hand, weaker downregulation leads to the formation of transient dauers (Gems et al., 1998; Patel et al., 2008). These observations

demonstrate that *daf-2* plays a role in regulating both dauer entry and dauer exit. The DAF-2 pathway also affects many other processes, including lipid metabolism and innate immunity (Kimura et al., 1997; Libina et al., 2003; Ludewig et al., 2004).

1.5 Insulin-like Peptides (ILPs) in *C. elegans*

Insulin-like peptides (ILPs) are short amino acid sequences that have structural similarities to the A and B chains of human insulin and insulin-like growth factor-1 (IGF-1) [Figure 1.6]. They are believed to bind to the DAF-2 receptor as ligands, although it is possible that they may also bind G-protein coupled receptors similar to the relaxin receptors found in humans (Allen et al., 2015). The *C. elegans* ILPs, which are expressed in neuronal and non-neuronal cells, are forty in number, which is much higher than that of more complex animals (Li et al., 2003; Pierce et al., 2001). For example, *Drosophila melanogaster* has 8 ILP genes (commonly known as dILPs) (Brogiolo et al., 2001; Rulifson et al., 2002), and humans have seven relaxins, two IGF's and an insulin, for a total of ten known ILP genes (Nef and Parada, 2000; Sherwood, 2004). The forty worm ILPs that are predicted to be ligands of the DAF-2 receptor have been found to have roles in various physiological processes, such as longevity, thermotolerance, learning, immunity, and others (Chen et al., 2013; Cornils et al., 2011; Fernandes de Abreu et al., 2014; Li et al., 2003; Pierce et al., 2001).

Based on structural predictions, the insulin-like peptides are classified into four different types, depending on the positioning of their disulfide bonds [Figure 1.6] (Pierce et al., 2001). Type γ ILPs have three disulfide bonds, all of them in canonical positions, similar to those of human insulin [Figure 1.6] (Pierce et al., 2001). Type α ILPs possess disulfide bonds in two of

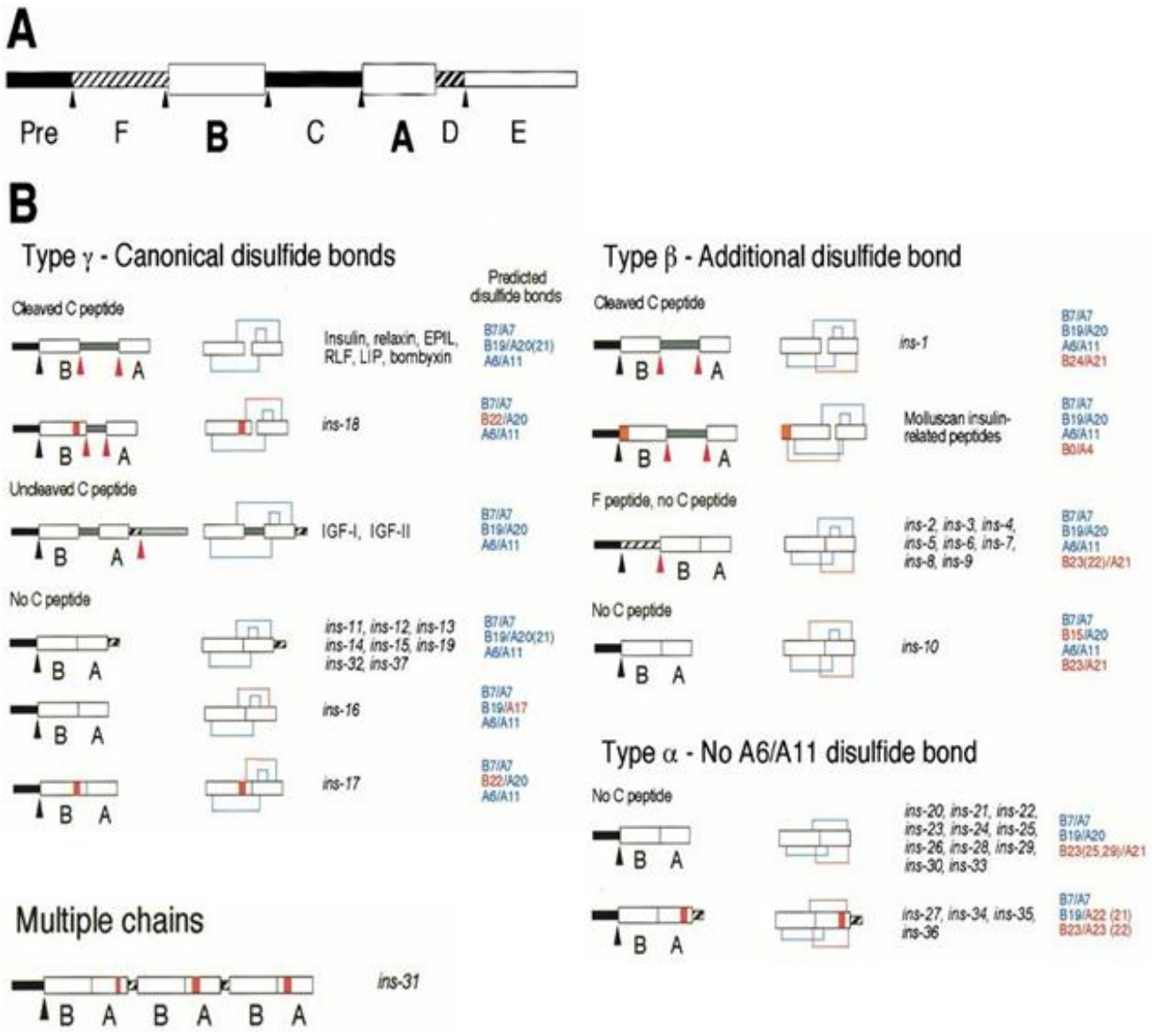

Figure 1.6 – Structural classes of the insulin-like peptides.
(A) Schematic of how the peptide chains of the ILPs might be arranged in *C. elegans*. Arrows represent sites where proteolytic cleavage can occur. (B) ILPs that are type γ have three disulfide bonds in the canonical positions in their structure. β-type ILPs have three disulfide bonds in similar positions as type γ ILPs, but they also possess a fourth disulfide bond located in a non-canonical position. Type α ILPs have two disulfide bonds in the canonical positions, with a third additional disulfide bond. (Taken from Pierce *et al*., 2001)
the canonical positions, with an additional third disulfide bond, whereas type β ILPs have three

canonical disulfide bonds, with a fourth disulfide bond in a non-canonical position [Figure 1.6]

(Pierce et al., 2001).

1.6 Insulin-like peptides influence development by processing sensory information

The DAF-2 receptor has been shown to act in the intestine, along with several head neurons (Apfeld and Kenyon, 1998; Wolkow, 2002), to mediate various physiological processes. Several ILPs have also been shown to be expressed in sensory neurons of the amphid region (Kodama et al., 2006; Li et al., 2003; Pierce et al., 2001; Tomioka et al., 2006). For example, *daf-28* is expressed in both the sensory neuron pairs ASI and ASJ in well-fed larvae, but is then downregulated by harsh environmental conditions, such as high dauer pheromone and low food (Li et al, 2003). Since the different ILPs are expressed from different subsets of sensory neurons, which could have different effects on the dauer program, it is possible that a particular subset of ILPs could be acting from a specific subset of sensory neurons to control worm physiology during different environmental conditions.

Cornils et al (2011) demonstrated that a combinatorial set of ILPs regulate dauer arrest and that the relative requirements of the ILPs differ between dauer entry and exit. During good environmental conditions, *daf-28* and *ins-6* promote reproductive development by inhibiting dauer entry, where *daf-28* plays a more important role (Cornils et al., 2011). These two ILPs also promote reproductive development by promoting dauer exit, where *ins-6* now plays a more dominant role in the process, compared to *daf-28* [Figure 1.7] (Cornils et al., 2011). Interestingly, *ins-6* regulates the two developmental switches in a cell-specific manner, where it acts from the ASI sensory neuron to inhibit dauer entry, but acts from the ASJ sensory neuron to promote dauer exit [Figure 1.7] (Cornils et al., 2011). On the other hand, during harsh conditions, *ins-1* acts to ensure dauer arrest by promoting dauer entry and inhibiting dauer exit (Cornils et al., 2011). Together these data demonstrate that specific ILPs can act combinatorially to regulate reproductive growth versus dauer arrest in response to the environment.

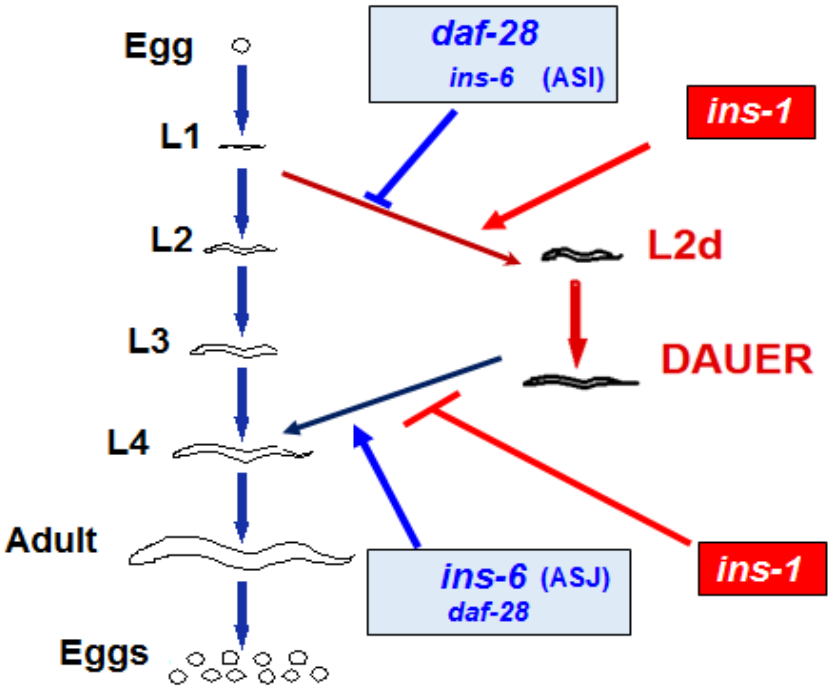

Figure 1.7 – The ILPs and sensory neurons involved in dauer development
During good environmental conditions, *daf-28* and *ins-6* both act to ensure reproductive growth. *daf-28* and *ins-6* both act from the sensory neuron ASI to inhibit dauer entry, while also acting in the sensory neuron ASJ to promote dauer exit. *daf*-28 plays a dominant role in inhibiting dauer entry in ASI compared to *ins-6,* while *ins*-6 plays a more dominant role in ASJ during dauer exit. During harsh conditions, *ins-1* acts to promote dauer entry and inhibit dauer exit, thereby ensuring dauer arrest. (Modified from Cornils et al, 2011).

1.7 The ILP-to-ILP Network

The high number of ILPs in *C. elegans* raises a question: why does an animal need so many ILPs? And how are each of the ILPs regulated? The Alcedo Lab, in collaboration with QueeLim Ch'ng's Lab in King's College (London, United Kingdom), used the single deletion mutants available for 34 of the 40 ILPs (Fernandes de Abreu *et al*, 2014) to determine their respective roles in dauer entry, dauer exit, and other physiological processes that are regulated by the DAF-2 pathway. They found that (1) not all the ILPs regulate the dauer program; (2) the set of ILPs that regulates dauer entry differ from the set of ILPs that regulates dauer exit, where some ILPs have stronger effects than others; and (3) among the ILPs that regulate dauer entry

or exit, the subset that inhibits a specific switch is also different from the subset that promotes the same switch [Figure 1.8] (Fernandes de Abreu *et al*., 2014). These data suggest that while there is some partial redundancy among some of the ILPs, they do function as a combinatorial code. Moreover, some ILPs can have dual opposing functions on the dauer program, *e.g.*, *ins-12* has a role in promoting both dauer entry and dauer exit [Figure 1.8], which suggests that some ILPs act as modulators depending on context cues (Fernandes de Abreu et al., 2014).

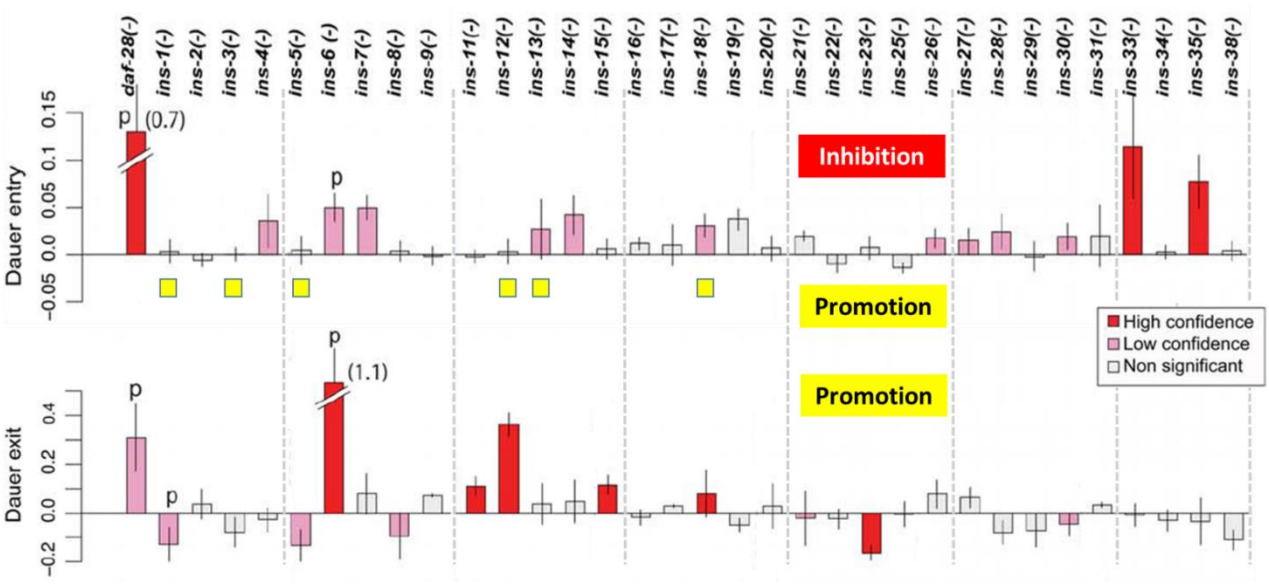

Figure 1.8 – The *C. elegans* ILPs interact as a combinatorial code to enhance survival
Top panel shows the dauer entry of available presumed null mutants of various ILPs. Bars in the positive value range indicate ILPs that inhibit dauer entry with different degrees of confidence. For example, the deletion mutants of *daf-28*, *ins-33*, and *ins-35* have red bars, indicating a high confidence value in inhibiting dauer entry under normal conditions, compared to wild type. Those that have negative values, like the ILPs denoted by the yellow boxes, are those that normally function to promote dauer entry. Mutations of these ILPs suppress the dauer formation phenotype of *daf-2(e1368)* or *daf-28(sa191*) mutants.

The bottom panel shows the ILPs that promote or inhibit dauer exit. Interestingly, the subsets of ILPs that inhibit dauer exit not only differ from those that promote dauer exit, but also from those that inhibit dauer entry. (Modified from Fernandes de Abreu et al., 2014)

This combinatorial code is presumably implemented by the ILP-to-ILP network organization of this peptide family. Indeed, qPCR and network analyses revealed that some ILPs promote and/or inhibit others and that the ILP network can be further organized into

several subnetworks [Figures 1.9 to 1.10] (Fernandes de Abreu et al., 2014). Interestingly, compared to most of the ILPs, *ins-6* has the most number of connections to other ILPs [Figures 1.9 to 1.10] (Fernandes de Abreu et al., 2014), which suggests that *ins-6* is a major node within the ILP-to-ILP network.

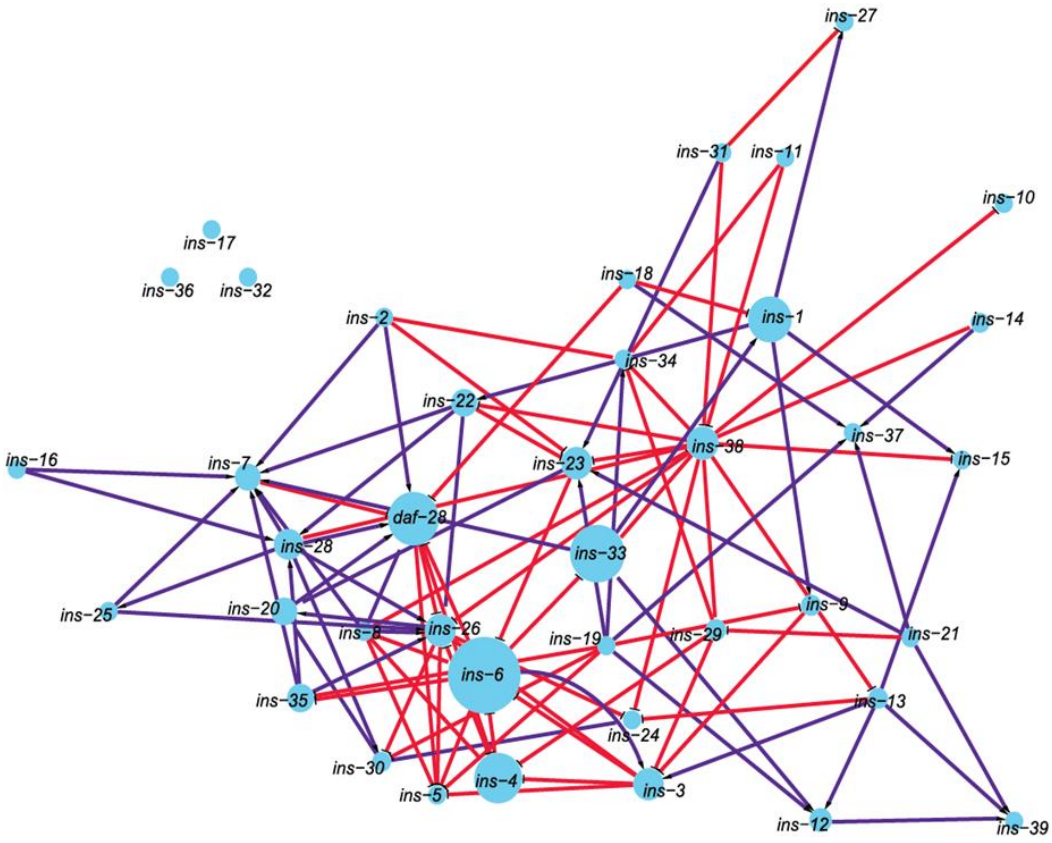

Figure 1.9 – The proposed ILP-to-ILP network
Lines in purple indicate connections where one ILP promotes the activity of another. Lines in red indicate connections where one ILP inhibits the activity of another. Circles in blue represent each of the ILPs, and are roughly scaled according to the number of connections it forms with other ILPs. For example, ILPs such as *daf-28* and *ins-33* connect to more ILPs that those of *ins-12* or *ins-25*. Not enough data was provided for *ins-17*, *ins-32*, and *ins-36* to position them confidently within the network. As shown, *ins-6* appears to be a very crucial node within the network (Fernandes de Abreu *et al,* 2014).

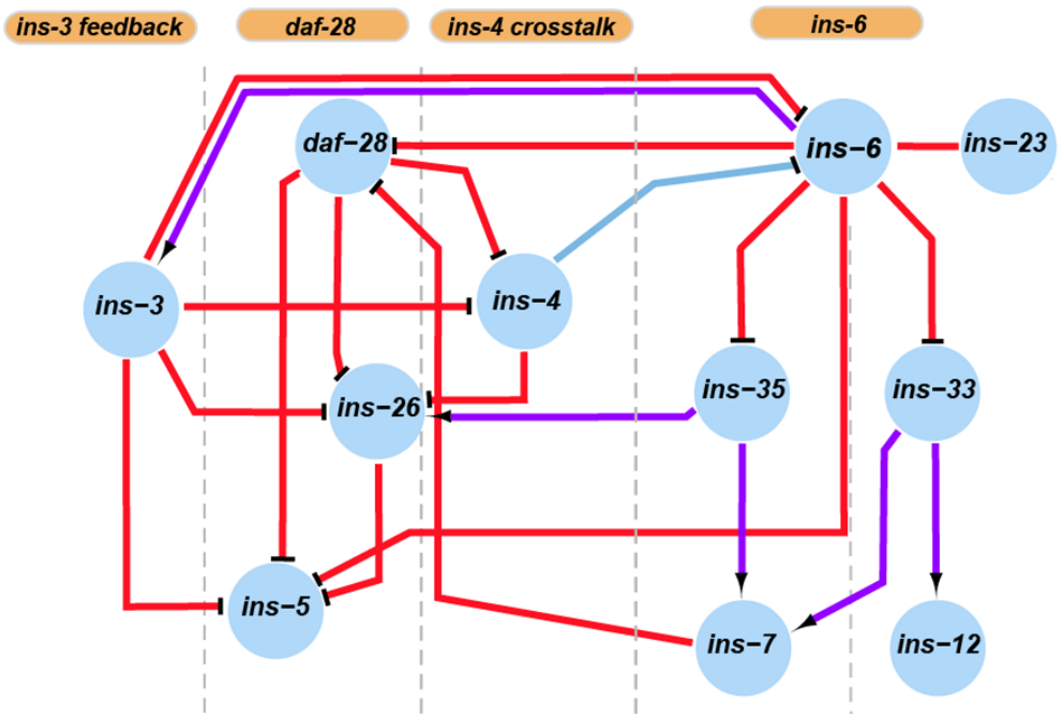

Figure 1.10 – An ILP-to-ILP subnetwork
Shown here is an ILP-to-ILP subnetwork for developmental plasticity. Two major branches are depicted, those of *daf-28* and *ins-6*. Depicted here is crosstalk, which acts through *ins-4*, and feedback between the two branches, which is provided through *ins-3* activity. Red lines indicate one ILP inhibiting another. Purple lines indicate one ILP promoting another ILP. Note that *ins-6* has the most number of connections to other ILPs within this subnetwork.

1.8 Endogenous expression pattern of *ins-6*

ins-6 mRNA is expressed in ASI and/or ASJ cell bodies in a stage-dependent manner [Figure 1.11] (Cornils *et al*., 2011; R. Chandra, personal communication). During L1, *ins-6* is expressed in low amounts only in the sensory neurons of ASI [Figure 1.11] (Cornils *et al.*, 2011; R. Chandra, personal communication). In late L2, *ins*-6 starts to be expressed in the ASJ cell body in a few worms [Figure 1.11] (R. Chandra, personal communication). By the L3 stage, *ins-6* is expressed in both the ASI and ASJ sensory neurons, with *ins-6* being more strongly expressed in ASI [Figure 1.11] (R. Chandra, personal communication). This pattern persists

through to the L4 stage, with *ins-6* being expressed in higher amounts in both neuron pairs compared to previous stages [Figure 1.11] (R. Chandra, personal communication). However, in dauers, *ins-6* in ASI gets turned off and *ins-6* is only present in ASJ [Figure 1.11] (Cornils *et al.*, 2011; R. Chandra, personal communication).

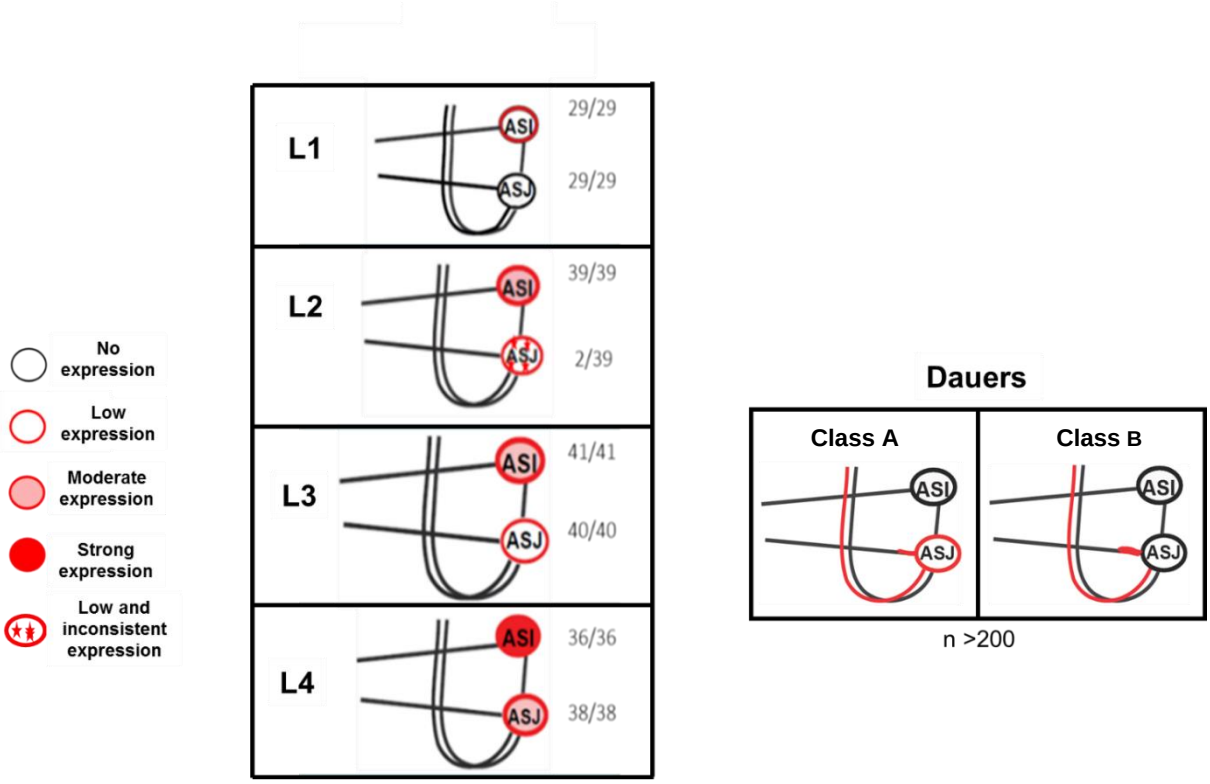

Figure 1.11 – The endogenous expression pattern of *ins-6* mRNA in well-fed animals and dauers.
During L1, *ins-6* mRNA is only expressed in low amounts in the sensory neuron ASI. However, by late L2, a few worms also begin to exhibit *ins-6* mRNA in the sensory neuron ASJ. By the L3 stage, *ins-6* mRNA is now localized in both sensory neurons of ASI and ASJ, with more *ins-6* mRNA being expressed in ASI. This pattern continues in the L4 stage, with both neurons exhibiting more *ins-6* mRNA than in L3. Interestingly, dauers have two classes of *ins-6* mRNA expression. Class A dauers have a high amount of *ins-6* mRNA in the ASJ cell bodies and a low amount in the ASJ processes, while Class B dauers have low *ins-6* mRNA expressed in the ASJ cell bodies and much higher amounts in the proximal and distal parts of the axon, which is located within the nerve ring. *ins-6* expression is determined by single molecule fluorescent in situ hybridization (smFISH) on wild-type animals using probes against *ins-6* mRNA. (R. Chandra, personal communication).

Intriguingly, there are two classes of dauers that show different *ins-6* mRNA subcellular localization [Figure 1.11] (R. Chandra, personal communication). In particular, class A dauers show a high amount of *ins-6* mRNA in the cell bodies of ASJ and a low amount in the processes, whereas class B dauers exhibit a low amount of *ins-6* mRNA in the ASJ cell body and a high amount of *ins-6* mRNA in the ASJ axon that leads into the nerve ring [Figure 1.11] (R. Chandra, personal communication). Quantitatively, class A dauers have a ratio that is equal or greater than 1 of *ins-6* mRNA in the ASJ cell body to *ins-6* mRNA in the nerve ring, and class B dauers have a ratio less than 1 of *ins-6* mRNA in the ASJ cell body to that in the nerve ring. These differing ratios of *ins-6* mRNA in the ASJ cell body and the nerve ring suggested that *ins-6* mRNA may be trafficked to the axons, raising the question about what regulates *ins-6* mRNA trafficking from the cell body to the axon and vice versa.

2. Thesis Scope

For my thesis, I aim to find the regulators of *ins-6* expression since it is a major node of the ILP-to-ILP network. The identification of its regulators should ultimately give insight into how the network is regulated. In particular, I want to determine how *ins-6* is regulated during dauer arrest under harsh environments versus its regulation during reproductive development under optimal environments. My studies should allow us to understand how *ins-6*, and ultimately how the network, coordinate different ILP activities in response to the environment and enhance survival.

To find the regulators of *ins-6*, I collaborated with two other members of the lab, Rashmi Chandra and Zahabiya Husain, in conducting a forward genetic screen. Through an ethylmethylsulfonate (EMS) screen of 2700 dauers, we pulled out five mutants that display wild-type *ins-6* expression during well-fed conditions, but have mutant *ins-6* expression during dauer arrest. These five mutants are categorized into three different classes based on their dauer-specific *ins-6* expression patterns.

We also took a candidate gene approach to find additional genes that affect *ins-6* mRNA localization during dauer development, which is the primary focus of my studies. Specifically, I

wish to know how *ins-6* mRNA is trafficked from the ASJ cell body to the nerve ring and vice versa. I looked at null or reduction-of-function mutants of worm kinesins, as possible regulators for *ins-6* mRNA trafficking, since kinesins are known to traffic cargo-like vesicles in *C. elegans* neurons. Of the possible neuronal kinesins, I, again in collaboration with Rashmi Chandra, have examined a subset and found three kinesin mutants that have different *ins-6* dauer mRNA levels and localization patterns compared to wild-type dauers. This suggests that the *ins-6* subcellular localization involves specific kinesins. Finally, this subcellular localization of *ins-6* is likely part of a post-transcriptional mechanism, where *ins-6* mRNA is locally translated in the axons due to altered communication between dauer neurons.

2. MATERIALS AND METHODS

2.1 Worm strains and culture

All worm strains used were maintained at 20°C for a minimum of two generations with abundant food on 6-cm nematode growth (NG) agar plates (Brenner, 1974). These plates were seeded with the *E. coli* strain OP50 as the food source.

The strains CB1265 [*unc-104(e1265)II]*, FF41 [*unc-116(e2310)III],* PT442 [*klp-6(sy511)III*; *him-5(e1490)V*], and RB2546 [*klp-4(ok3537*)*X*] were obtained from the Caenorhabditis Genetics Center (CGC), Minneapolis, MN. *unc-104(e1265)II* was outcrossed to the QZ186 [*mgIs40(daf-28p::gfp)*] strain five times to mark both ASI and ASJ cell bodies and the *e1265* point mutation (www.wormbase.org) was followed by PCR (see primer sequences below). On the other hand, *klp-4(ok3537*)*X* was outcrossed six times to wild type (QZ0, the Alcedo lab N2 strain) to remove background mutations and also outcrossed to the QZ186 strain to mark both ASI and ASJ cell bodies, whereas *klp-6(sy511)III* was only outcrossed to QZ0 six times. The *ok3537* deletion and the *sy511* point mutation (www.wormbase.org) were again followed by PCR (primer sequences are below). Since the *unc-116(e2310)III* strain has yet to be curated, outcrossing was done six times to QZ0 or QZ186 by following the known *e2310* phenotypes: strongly uncoordinated (Unc) larvae and mildy dumpy (Dpy) and Unc adults (www.wormbase.org).

2.2 Primers used for genotyping

klp-4(ok3537)X

To detect the ~600 bp-deletion in *klp-4* mutants, the following primers used are:

klp-4 fwd2: 5'- TTG ACT GGA CAT ACC GC - 3'

klp-4 outer rev-R: 5'-CAC TTG TCG GGT ACG AAT CAA G- 3'

To detect single nucleotide differences between wild type and mutant strains, the nucleotide at the 3’ end (bold-faced) of the forward primers was designed to match either the wild-type (WT) or the mutant (MUT) nucleotide. To increase the efficiency in detecting the single nucleotide

difference between wild type and mutant, the nucleotide at the third position from the 3' end (underlined) was mutated in the two forward primers (Maier and Neagu, 2011).

klp-6(sy511)III

klp-6 WT fwd: 5'-ATT GCG TCT TCT GTC GTA TTT TCG **C** -3'

klp-6 MUT fwd: 5'-ATT GCG TCT TCT GTC GTA TTT TGG **T** -3'

klp-6 reverse: 5'-CAC GGG GAG AGA CCT ACT GT - 3'

unc-104(e1265)II

unc-104 WT F-primer: 5' - TTC TTT TAT TCC GTG ATG ATC TA**G** - 3'

unc-104 MUT F-primer: 5' - TTC TTT TAT TCC GTG ATG ATC AA**A** - 3'

unc-104 Rev-primer: 5' - ATT GAG GCC AGG CTT CAC - 3'

2.3 Solutions

Hybridization buffer that contains 15% formamide (10 mL)

This solution was prepared using the following: 1 g dextran sulfate, 10 mg *E. coli* tRNA (New England Biolabs, Inc.), 100 µL of 200 mM vanadyl ribonucleoside complex (New England Biolabs, Inc.), 40 µL of 50 mg/mL RNase-free bovine serum albumin (BSA, Ambion), and 1.5 mL deionized formamide (Ambion). Nuclease-free water (Ambion) was added to a final volume of 10 mL. The resulting buffer is mixed gently, using a nutator at room temperature, and then stored in a -20° C freezer.

2X Saline Sodium Citrate (SSC) buffer

The 2X SSC solution was prepared from 20X SSC buffer solution ordered from Ambion. This 20X solution contained 3.0 M sodium chloride and 0.30 M sodium citrate, and was passed through a 0.2-µm filter.

Wash buffer (50 mL)

Wash buffer was prepared using the following: deionized formamide (Ambion) at the same concentration as the hybridization buffer and 5 mL of 20X SSC (RNase-free, Ambion).

Nuclease-free water (Ambion) was added to a final volume of 50 mL. The buffer is stored at room temperature.

S Basal buffer (1 L)

This buffer (modified from Golden and Riddle, 1982) was made with 5.85 g NaCl, 1 g K_2HPO_4, and 6 g KH_2PO_4, followed by addition of distilled, deionized water to a final volume of 1 L. The buffer is then autoclaved; after it cooled to room temperature, 1 mL of a 5 mg/mL cholesterol solution (in ethanol) was added

S medium

The S medium (modified from Golden and Riddle, 1982) used to prepare crude dauer pheromone was made accordingly: 1 L S-Basal buffer, 10 mL 1 M potassium citrate (pH 6.0) [20 g citric acid monohydrate; 293.5 g tri-potassium citrate monohydrate; distilled, deionized water to a final volume of 1 L; then autoclaved], 10 mL trace metals solution [1.86 g disodium EDTA; 0.69 g $FeSO_4$•$7H_2O$; 0.2 g $MnCl_2$•$4H_2O$; 0.29 g $ZnSO_4$•$7H_2O$; 0.025 g $CuSO_4$•$5H_2O$; distilled, deionized water to a final volume of 1 L; then autoclaved and stored in the dark at room temperature], 3 mL 1 M $CaCl_2$, and 3 mL 1 M $MgSO_4$.

2.4 Chemical mutagenesis

The chemical mutagenesis of *C. elegans* was done according to Anderson (1995), with some modifications. About two hundred L2/L3 larvae from the QL285 strain [*ttTi5605 drcSi68(ins-6p::mCherry; Cb-unc-119*[+]*)II*], also known as *Pins-6::mcherry*, were transferred onto each 10-cm NG agar plate, where four plates were prepared. Upon the next day, the resulting gravid adults were bleached to recover their eggs, and the eggs were transferred into a 15-mL Falcon tube and washed three times with 5 mL M9 buffer (Brenner, 1974). The egg pellet was subsequently resuspended in 400 µL of M9 buffer, where 100-µL suspensions were then each aliquoted onto four 10-cm plates. The eggs were allowed to grow to the early L4 stage and then subjected to a final concentration of 50 mM ethyl methanesulfonate (EMS) for 4 hours at 20°C

to introduce random point mutations into the genome. Worms were recovered overnight at 15°C. They were then separated, where every set of five L4s was transferred onto each of the ten 6-cm plates and kept at 20°C. Mutagenized parents were transferred every six hours so that any laid progeny were not crowded. Worms were allowed to propagate to the F2 generation, which were then starved for dauer formation. By using a fluorescent dissecting scope, 2700 F2 dauers were screened for mutants with different *ins-6* expression from wild-type worms [Figure 2.1]

A secondary screen was done on the mutants to look for those that had mutant dauer *ins-6* expression, but wild-type *ins-6* expression during well-fed non-dauer larval stages.

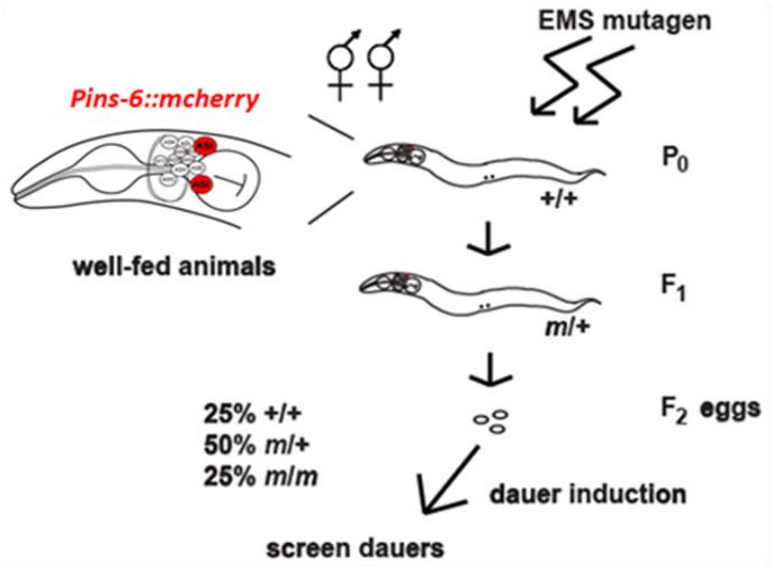

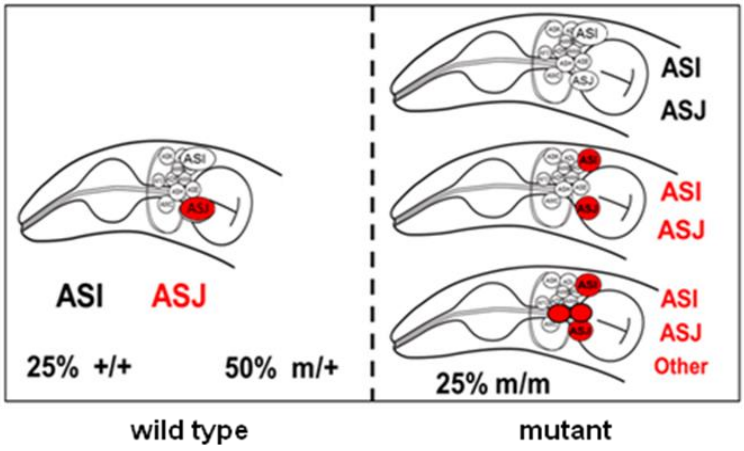

Figure 2.1 – Schematic of the EMS screen
Pins-6::mcherry worms were mutagenized with ethyl methanesulfonate (EMS) and allowed to progagate to the F2 generation. About 2700 F2 dauers were then screened for mutant dauer *ins-6* expression compared to wild-type worms.

2.5 Dauer entry assay

About 20-30 gravid adults were picked and transferred to a separate plate seeded with OP50. These adults were allowed to lay eggs for 2-4 hours, which would be enough time to allow over 100 eggs to be laid. Eggs were then transferred to new OP50 plates, with approximately 50 eggs per plate. Plates were transferred to a 27°C incubator at a relative humidity of ~20% (in the absence of a humidifier) or ~50-60% (in the presence of a Vicks humidifier, model V3100, 1 gallon volume on high setting). Twenty-four hours after egg transfer, the plates were checked for worms that had undergone L1 arrest. Forty-eight hours after egg transfer, plates were checked for L1 arrest and/or dauer formation.

2.6 Dauer exit assay

Worms were kept at 20°C and allowed to starve to form dauers. Over a hundred 5-day-old dauers were placed onto 6-cm plates containing OP50. The number of dauers versus the number of animals that exited into the L4 stage was scored every six hours. After scoring the post-dauer animals, these animals were killed to prevent progeny contamination that can arise if these animals were allowed to continue to reproductive adulthood. The assay continued until all worms exited dauer arrest.

2.7 Fixation of worms

The fixation of worms was done according to Ji and van Oudenaarden (2012), with some modifications. Worms were maintained at 20°C for a minimum of two generations on three or more 6-cm NG agar plates with abundant *E. coli* OP50. Once they reached the desired stage, worms were washed with approximately 5 mL of water or M9. The worms were transferred to a 15-mL Falcon tube and centrifuged at 3000 rpm for 5 minutes, after which a pellet of worms

become visible. The supernatant was removed, and the worms were washed a second time with water. The pellet of worms was then transferred to a 1.5-mL Eppendorf tube, to which 1 mL of 4% paraformaldehyde (PFA) in a phosphate-buffered saline solution (PBS) was added. The worm suspension was subsequently mixed gently in the 4% PFA solution for 45 minutes at room temperature, using a nutator, after which the worms were washed twice with approximately 1 mL of 1X PBS to remove residual PFA. The worm pellet was resuspended in 70% ethanol and the worm suspension was gently mixed overnight at 4°C, by again using a nutator. Worms were stored in 4°C for up to 3 weeks.

2.8 Small molecule fluorescent *in situ* hybridization (smFISH) of worms

We followed the smFISH protocol of Ji and van Oudenaarden (2012) with some modifications. We only used fixed samples that were less than 3 weeks old, which were pelleted by centrifugation at 3000 rpm for 5 minutes to remove the 70% ethanol. Worms were then washed with 1 mL of wash buffer and allowed to stand for 2-5 minutes before centrifugation. After aspiration of the wash buffer, 500 µL of hybridization buffer was added to the worms in the dark, along with 1 µL of the *ins-6* probe (Stellaris, Petaluma, CA), to a final probe concentration of 1:500. Worms were hybridized overnight at 30°C for 16-17 hours using a nutator, after which worms were spun down and the hybridization buffer was removed. Next, worms were washed with 1 mL of wash buffer and mixed gently on a nutator at 30°C. The wash buffer was changed about every 1.5 to 2 hours with 1 mL of wash buffer each time, for a total of about 4-5 washes during the first day of washes at 30°C. After the last wash, the worms were again incubated overnight at 30°C on a nutator. This was followed by a second day of washing, which could be 2 to 3 washes every 3 hours and could be further extended for a second overnight of washing at 30°C. After the washes were done, the worms were placed in 2X SSC. Worms were then stored in 4°C for up to three weeks before being analyzed on a 1% agarose pad.

2.9 *ins-6* probe specifications

The following oligo sequences were designed against the *ins-6* spliced transcript sequence ZK84.6 (www.wormbase.org) and labeled with a CalFluor 610 probe. The probes were ordered through Stellaris (Petaluma, CA).

Probe #	Probe (5' → 3')	Probe Position	Percent GC
1	ttggagtgcgcacaaaacga	28	50.0%
2	attgacggaaacttgcagcg	50	50.0%
3	tcagacattgaaggaccgaa	72	45.0%
4	aagttgcatgcttgctgatt	94	40.0%
5	tgttgtgttgaagttcacgg	116	45.0%
6	attggtcggtgagctgattc	141	50.0%
7	tggaacacgtcttgctcgtg	163	55.0%
8	agatgagttttcttccgcag	203	45.0%
9	ccacagacagccatgactaa	225	50.0%
10	ttcttgtgggttgcaaagat	247	40.0%
11	attcagtcgcaatgtccttt	269	40.0%
12	atcagaacactgatttccgc	292	45.0%
13	catggacaacaagcagatct	321	45.0%
14	ggtacagagactgatatcgg	357	50.0%
15	cacgggtgaaacgagattca	394	50.0%
16	tgggatgacagatttgatga	416	40.0%
17	caaggtttattgtacaagcc	438	40.0%

2.10 smFISH image analysis

Endogenous *ins-6* expression is quantified according to the probes' combined fluorescence intensities, where the background intensities were subtracted, using the software Nikon NIS Elements version 4.51. For nerve ring intensity measurements, the entire area of the structure was measured, since the signal was diffuse. For signals that appear punctate and perinuclear, like those around the ASJ cell body, only the punctate, perinuclear areas were taken into account.

Worms with high *ins-6* expression in the ASJ cell body and low *ins-6* expression in the nerve ring are classified as Class A dauers (ratio ≥ 1). Worms with a ratio < 1 are classified as Class B dauers.

2.11 Crude Dauer Pheromone Preparation

This preparation is according to Nika et al. (2016) with some modifications. Wild-type adult worms were bleached to remove any contaminations and to synchronize the growth of larvae. Bleached plates were chunked and propagated onto at least 15 to 20 6-cm plates seeded with OP50. These worms were kept at 20°C until the food was almost gone on all plates. To harvest, the plates were washed with 5 mL of S medium and the worms were collected into a 15-mL Falcon tube. Worms were counted in three 10 µL drops to estimate population density. At least 90,000 worms were added per 150 mL of S Basal and/or S medium in Erlenmeyer flasks. The culture of worms was shaken at 22.5°C to 25°C at 225 rpm for 9 days. Worms were fed 3 mL of 25X OP50 stock per 150 mL on day 0, 1 mL on day 1, and 3 mL on days 2 through 8. On day 9, cultures were divided into 50 mL Falcon tubes and centrifuged to collect the supernatant of interest. All collections of supernatant were pooled together and brought to a boil on a heating plate with a stir bar to reduce the suspension down to a yellow paste and/or crystals. A hair dryer was also used to accelerate the evaporation process.

To extract the pheromone mixture out of the paste and/or crystals, 50 mL 195 proof ethanol was added to the beaker, which was shaken at 250 rpm for at least 2 hours to overnight. This extraction was done up to six times, or until the extracts no longer appeared yellow in color. Extracts were filtered through a Whatman paper and stored at 4°C until all extracts were obtained. The filtrates were combined and evaporated down to approximately 1-3 mL, which would at this point consist of an oily residue and precipitates on the outer wall of the beaker. The oily residue was collected and stored in an Eppendorf tube, while the precipitates were dissolved with autoclaved water and collected in a separate tube. For testing, 50 µL of crude pheromone was used on 3-cm plates of NGM that were seeded with 20-30 µL of OP50 in the presence or absence of bactopeptone. The 50-µL volume either consisted of all oily residues, all dissolved precipitates, or a ratio of both substances.

3. RESULTS

3.1 – A forward mutagenesis screen to find regulators of the ILP *ins-6*

Our previous study suggested that *ins-6* is an important node within the ILP-to-ILP network in *C. elegans* (Fernandes de Abreu, 2014). Thus, to understand how the network is regulated, we wanted to elucidate the regulators of *ins-6* during development, specifically during dauer arrest. The identification of specific regulators of *ins-6* during the dauer stage, a form of developmental plasticity under harsh conditions, would also presumably provide insight into how the network optimizes animal survival in response to changing environments.

One approach we undertook was to conduct a forward genetic mutagenesis screen (Anderson, 1995). We took a *C. elegans* strain carrying a *Pins-6::mcherry* transcriptional reporter that closely reflected the endogenous *ins-6* mRNA expression pattern in well-fed and dauer-inducing conditions, and subjected a population of these animals to ethyl methanesulfonate (EMS). The EMS mutagen introduced random point mutations and/or small insertions/deletions into the germline of these animals. After mutagenesis, these worms were allowed to reproduce for two generations, *i.e.*, till the F2 generation. F2 dauers were then screened for altered *ins-6* expression patterns [Figures 2.1 and 3.1].

Wild-type dauers turn off *ins-6* expression in the dauer-inhibiting sensory neuron ASI, but express *ins-6* only in the sensory neuron ASJ [Figures 2.1, 3.1 and 3.2A] (Cornils *et al.*, 2011; R. Chandra, personal communication). Hence, of the mutant dauers we isolated, we classified them into three different groups [Figures 2.1, 3.1 and 3.2]: (i) class I, where the mutants do not turn off *ins-6* expression in ASI; (ii) class II, where the mutants have reduced or no expression in the sensory neuron ASJ; and (iii) class III, where the mutants express *ins-6* ectopically in other neurons, besides ASI and ASJ. These mutant dauers were then additionally screened for wild-type or mutant *ins-6* expression in well-fed, non-dauer larvae, where only mutants that displayed

mutant dauer-specific *ins-6* expression, but wild-type non-dauer *ins-6* expression were further characterized [Figure 3.1].

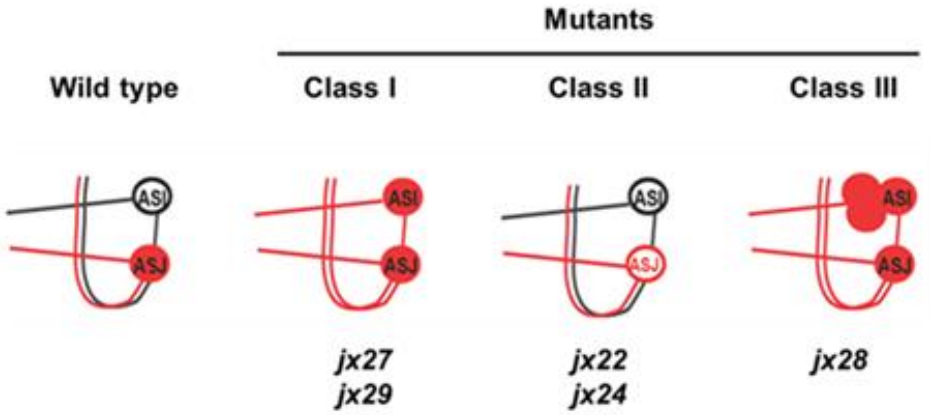

Figure 3.1 – A schematic of the three classes of five mutants obtained from the EMS screen
Wild-type dauers do not express *ins-6* in ASI neurons (open black circle), but express *ins-6* in ASJ neurons (closed red circle). Class I mutants *jx27* and *jx29* express *ins-6* in both ASI and ASJ (closed red circles). Class II mutants *jx22* and *jx24* have lower amounts of *ins-6* expressed in the ASJ cell body compared to wild type (open red circle). Class III mutant *jx28* has *ins-6* in both ASI and ASJ neurons, as well as additional neurons (closed red circles).

After screening approximately 2700 F2 dauers, five mutants were isolated. *jx27* and *jx29* represent Class I mutant dauers, with *ins-6* expressed in both ASI and ASJ neurons [Figures 3.1 and 3.2]. Class II dauers are represented by mutants *jx22* and *jx24* and have lowered expression in the neuron ASJ compared to wild-type animals, whereas Class III dauers are represented by mutant *jx28*, which has *ins-6* expressed in several neuron pairs that include ASI and ASJ [Figures 3.1, and 3.2].

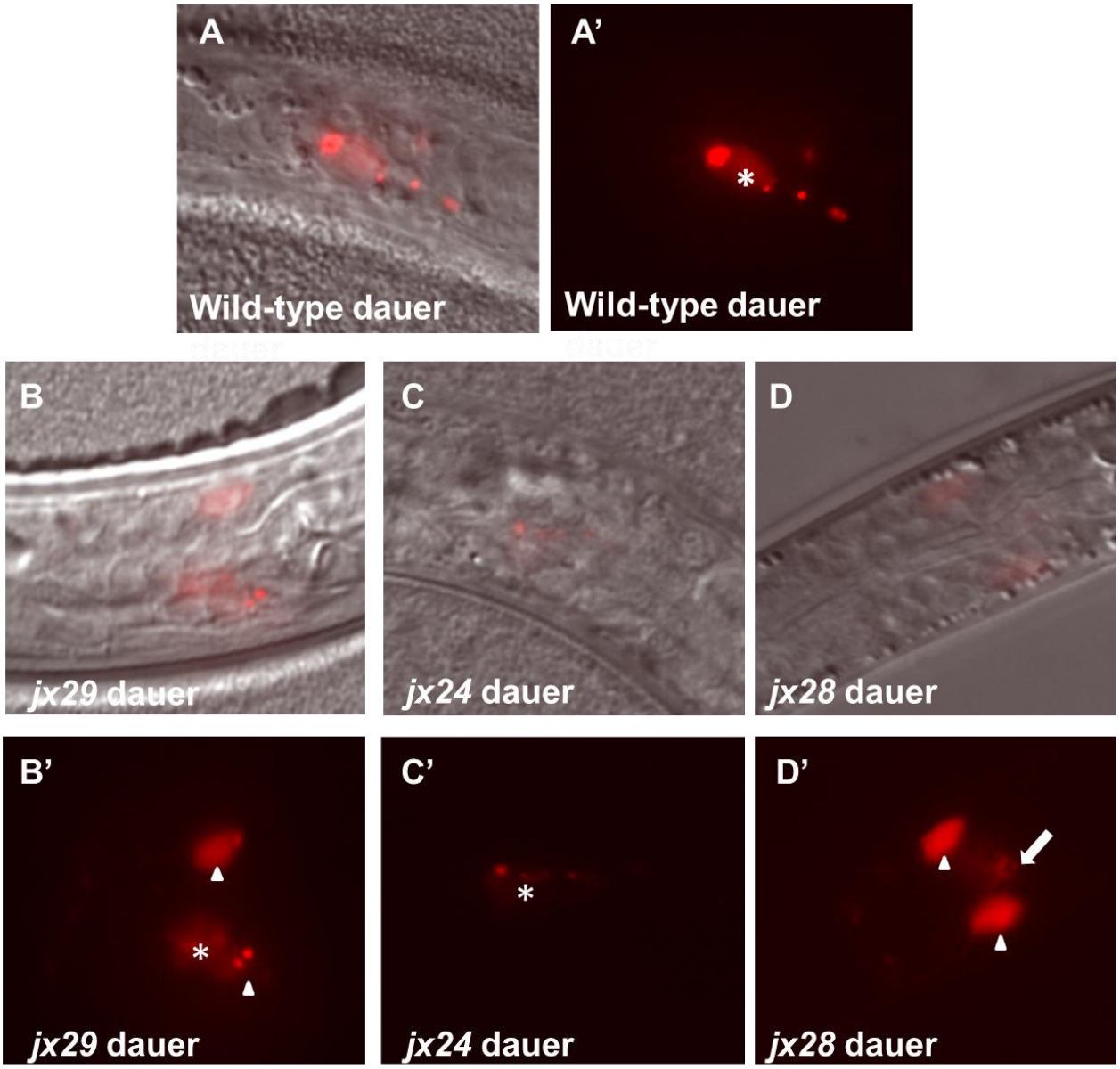

Figure 3.2 – DIC and fluorescent images of the three mutant classes

(A and A') A wild-type dauer with *Pins-6::mcherry* in ASJ (asterisk). (B and B') *jx29*, a Class I dauer mutant, which expresses *Pins-6::mcherry* in both ASI (arrowheads) and ASJ (asterisk). (C and C') *jx24*, a Class II dauer, exhibits lowered *Pins-6::mcherry* in ASJ (asterisk), compared to wild-type dauers. (D and D') *jx28*, a Class III dauer, expresses *Pins-6::mcherry* in ASI (arrowheads) and ASJ (not shown), along with a third unknown neuron (arrow). Panels A-D show DIC images overlaid with the corresponding red fluorescent images. Panels A'-D' show the fluorescent images by themselves. All animals are shown with their anterior side to the left and their dorsal side up, with the exception of *jx28* in panels D and D'. Instead of lying on its lateral side, like the other animals, this *jx28* animal is lying on its dorsal or ventral side.

3.2 – Only *jx24* and *jx29* display dauer phenotypes

We tested the five EMS mutants for dauer entry phenotypes. *jx24* is the only mutant that has a statistically significant increase in dauer formation, with 10-15% more worms entering dauer arrest compared to control worms [Figure 3.3].

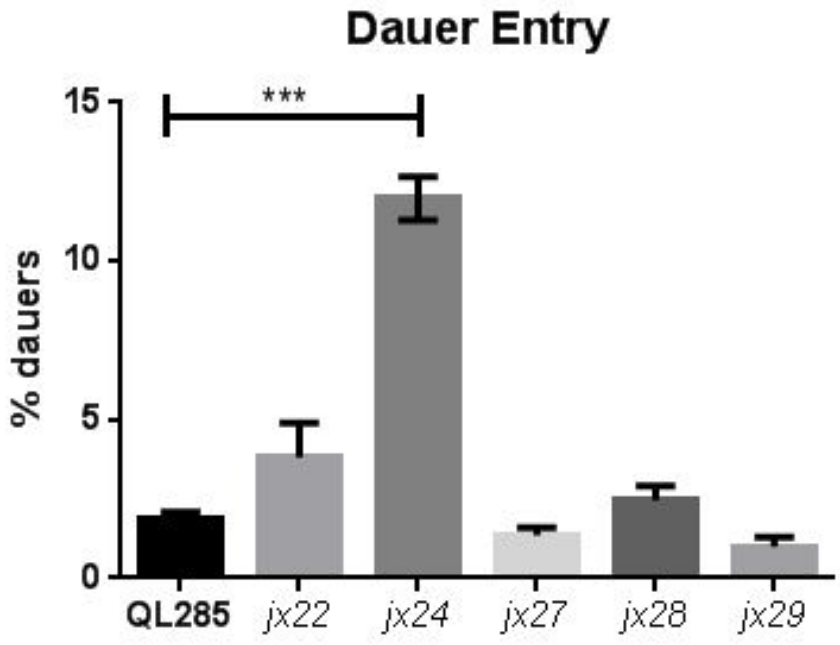

Figure 3.3 – Dauer entry results of the EMS mutants
The five mutants pulled from the EMS screen were tested for dauer entry phenotypes against the control, the *Pins-6::mcherry* parent strain (QL285). Only *jx24* had a significant difference from control worms in the percentage of dauers formed (***, p = 0.0003). Error bars represent standard error. One-way ANOVA with Bonferroni was used.

We also tested the EMS mutants for dauer exit phenotypes. Only two mutants showed a difference in exit rate compared to control worms: *jx24* and *jx29.* Both of these mutants were delayed compared to controls [Table 3.1].

Mutant	**Log-Rank**	**Wilcoxon**
jx22	0.05	0.11
jx24	**0.0003**	**0.0006**
jx27	0.439	0.324
jx28	0.2319	0.2797
jx29	**0.0004**	**0.0004**

Table 3.1 – Dauer exit results of the EMS mutants.
The above table shows p values compared to control worms after performing both log-rank and Wilcoxon tests when α = 0.05. Only *jx24* and *jx29* both have statistically significant delays in dauer exit compared to the parent strain (in red bold face).

Our screen produced 3 different classes of mutations that not only had distinct effects on *ins-6* dauer-dependent expression, but also had distinct effects on developmental plasticity. Since *ins-6* acts from ASJ to promote dauer exit (Cornils et al., 2011), it is not surprising that the class II mutation *jx24* had a delayed dauer exit phenotype [Table 3.1], because *jx24* downregulated *ins-6* in ASJ of dauers [Figures 3.1 and 3.2]. However, among the *jx* mutations that we had so far isolated, we also had (i) a class I mutation (*jx29*) that had no effect on the dauer expression of *ins-6* in ASJ [Figures 3.1 and 3.2], but delayed dauer exit [Table 3.1]; and (ii) a class II mutation (*jx22*) that downregulated *ins-6* in ASJ of dauers [Figure 3.1], but in this

case had no effect on dauer exit [Table 3.1]. Moreover, we isolated the class II mutation *jx24* that does not affect *ins-6* expression in ASI [Figures 3.1 and 3.2], the sensory neuron from which this ILP acts to inhibit dauer entry, yet this mutation did exhibit a dauer entry phenotype [Figure 3.3]. Thus, these observations together suggest that the mutations from our EMS screen were not targeting *ins-6* expression indirectly by simply regulating dauer entry or exit.

3.3 – Humidity may also influence dauer entry

Often when conducting dauer entry assays, we used a *daf-28(tm2308)* null mutant as a positive control, since it has a high dauer-entry phenotype at 27°C. Previous results from the lab in Basel, Switzerland, and our collaborators in London, England, showed that 50-80% of *daf-28(tm2308)* animals entered dauer arrest at 27°C (Cornils et al., 2011; Fernandes de Abreu et al., 2014). However, whenever lab members at Wayne State tested the same *daf-28* null mutant, less than 50% of the *daf-28* mutants entered dauer arrest. Upon exploring possible environmental differences, which could lead to the variability in dauer entry phenotypes, we noted the differences in the humidity of the labs. For example, in the month of June during one of the experiments in Detroit, the relative humidity of the lab is around 20%, while the relative humidity of the lab in Basel in June, around the same time of a similar dauer entry experiment is 50-60% (M. Regenass, J. Alcedo, data not shown).

I tested the effect of low humidity versus high humidity on the dauer formation of both wild-type and *daf-28* mutant worms. To induce high humidity, I placed a humidifier that holds 1 gallon of water in the incubator and set it to high, leading to a relative humidity of around 55% inside the incubator. Interestingly, high humidity at 27°C decreases embryonic arrest and L1 arrest, but increases dauer arrest, in contrast to low humidity [Figure 3.4], which suggests that dauer entry is modulated by humidity in the environment.

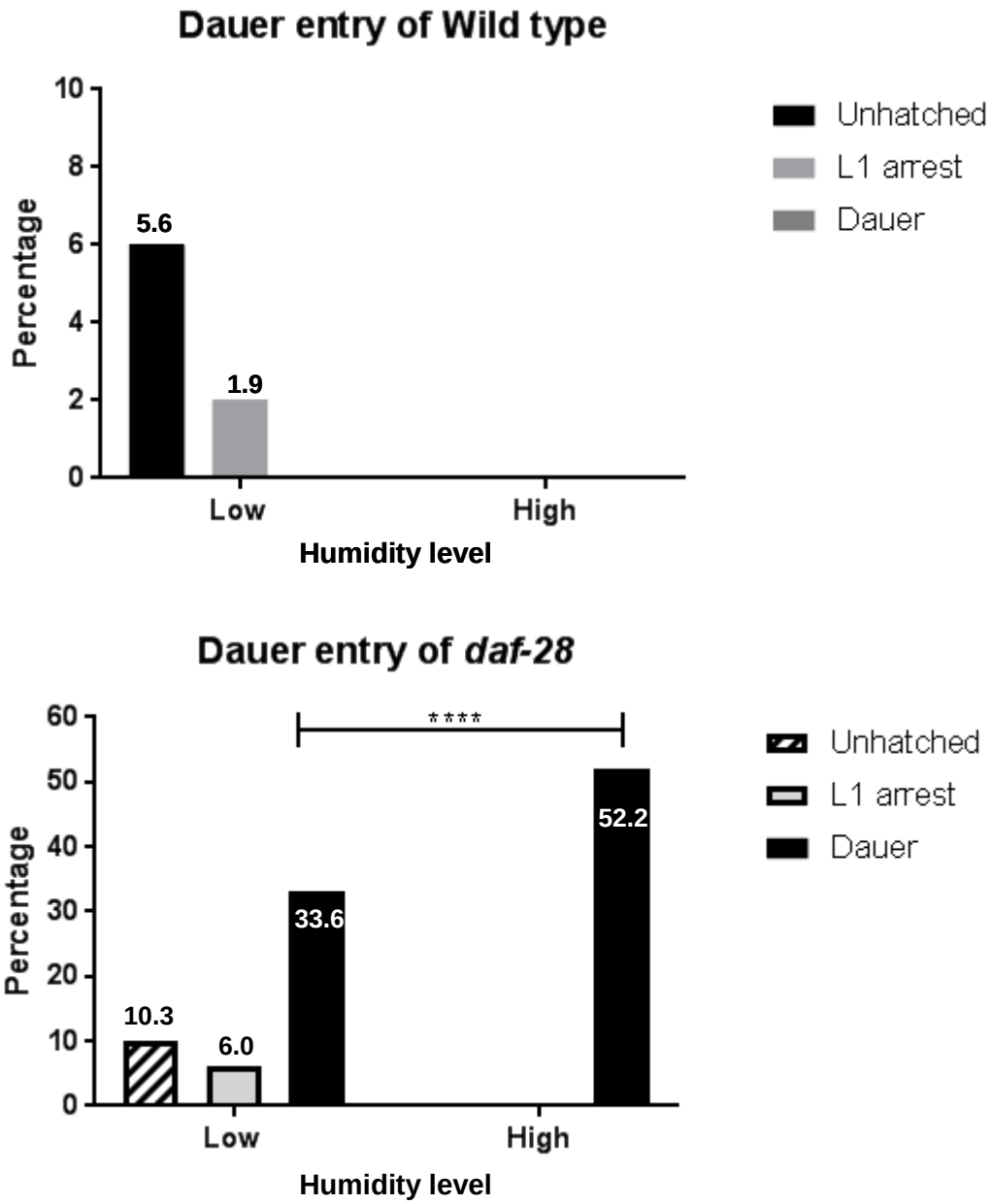

Figure 3.4 – Percentage of unhatched embryos, L1 arrested animals, and dauer-arrested animals in low versus high humidity conditions

Top graph shows the phenotypes of wild-type worms (n = 101), which serve as a negative control for dauer entry. They have a low percentage of unhatched embryos and L1 arrest in low humidity conditions (relative humidity ~25%). In high humidity conditions (relative humidity ~55%), all animals developed normally through the different stages. Similar to wild-type worms, *daf-28(tm2308)* null mutants (n = 47) shown in the bottom graph no longer exhibit any embryonic arrest or L1 arrest under high humidity conditions. However, the number of dauers formed increases significantly from ~35% to ~50% when comparing low versus high humidity conditions, respectively, p=0.0006, chi-square test.

My findings above [Figure 3.4] may also explain the low potency of my crude dauer pheromone preparations compared to those made in Switzerland. Previous pheromone preparations caused ~45-55% complete dauer formation at 25°C within two days, when 100-200 μl of the pheromone prep was added to 3.5-cm NG agar plates that also contain 50 μl of *E. coli* OP50 and ~100 embryos (Cornils et al., 2011). My best pheromone preps only produced transient dauers within three days and at lower percentages (16% and 26% complete dauer formation in two different trials). Thus, it is possible that humidity could also regulate the synthesis and/or secretion of a component of the dauer pheromone mixture secreted by the animal throughout its life, and that high humidity during the pheromone preparation could increase the dauer-inducing potency of the pheromone.

4. A candidate gene approach to find regulators of *ins-6* mRNA

During dauer arrest, *ins-6* mRNA displays different subcellular localizations: in the ASJ cell body versus the distal parts of the axons in the *C. elegans* nerve ring (R. Chandra, personal communication). This was intriguing as it suggested that *ins-6* undergoes post-transcriptional regulation, where *ins-6* mRNA has to be locally translated in the axons to enhance the animal's survival. To determine the mechanism behind this process, I aimed to identify some of the proteins that regulate *ins-6* mRNA trafficking in dauers. To do so, I focused on the effects of several neuronally-expressed kinesins, a number of which have been implicated in trafficking cargoes in an anterograde direction, while some have been shown to traffic cargoes in a retrograde direction (Encalada et al., 2011; Maday et al., 2014; Roostalu et al., 2011; Schuster et al., 2011).

4.1 – Wild type has two classes of dauers

Wild-type dauers display two classes of *ins-6* mRNA subcellular localization within the ASJ sensory neurons, as demonstrated by small-molecule fluorescent *in situ* hybridization (smFISH) of *ins-6*. Class A dauers have more or the same levels of *ins-6* mRNA in the ASJ cell bodies than in the distal parts of the axons, which means that their *ins*-6 mRNA ratio in the ASJ soma to the nerve ring is equal to or greater than 1. In contrast, class B dauers display less *ins-6* mRNA in the ASJ cell bodies and more in the axons of the nerve ring, making their *ins-6* mRNA ratio in the ASJ cell body to the nerve ring less than 1 [Figure 4.1] (R. Chandra, personal communication). The wild-type dauers are roughly evenly distributed between class A and class B [Table 4.1].

To confirm that the *ins-6* mRNA we observed in the nerve ring was not an artifact of fixation or nonspecific binding of the *ins-6* probe, my collaborator R. Chandra and I also performed *ins-6* smFISH on the *ins-6(tm2416)* deletion mutants with every experiment. *ins-6*

deletion null mutants showed significantly less or no *ins-6* mRNA in the nerve ring and do not have any *ins-6* mRNA in the ASJ cell body [Figure 4.2].

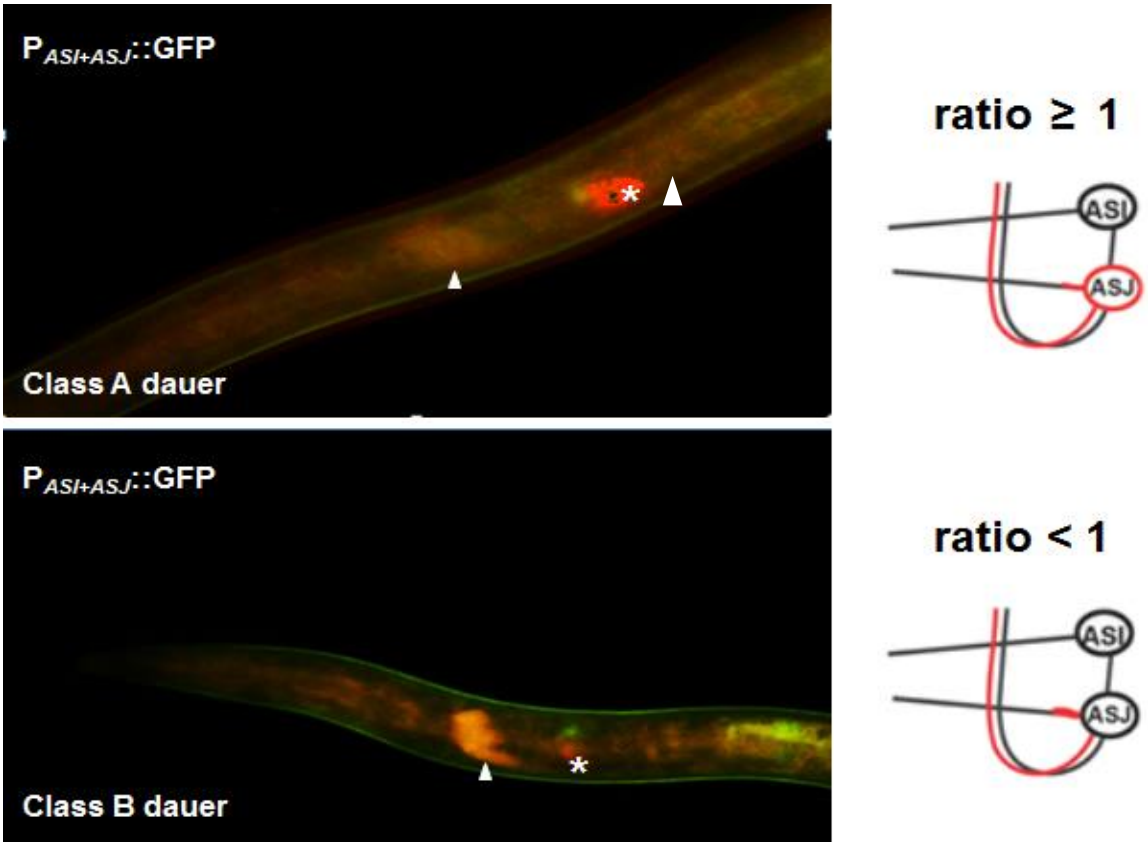

Figure 4.1 – Two classes of *ins-6* mRNA subcellular localization are observed in wild-type dauers after *ins-6* smFISH.
The top and bottom images on the left represent *ins-6* smFISH performed on a strain that marks both ASI and ASJ neurons with GFP, which are represented as simplified drawings on the right. *ins-6* mRNA is fluorescently labeled in red. The top left panel shows a wild-type class A dauer, where *ins-6* mRNA is present in higher amounts in the ASJ cell body (asterisk), compared to the nerve ring (arrowhead). Class A dauers thus have a ratio of ≥ 1 of *ins-6* mRNA in the ASJ soma versus the nerve ring (top right panel). The bottom left panel shows a wild-type class B dauer, where *ins-6* mRNA is now seen less in the ASJ cell body (asterisk) and more in the nerve ring (arrowhead). Class B dauers thus have a ratio of < 1 of *ins-6* mRNA in the ASJ soma versus the nerve ring (bottom right panel). Animals are arranged with their anterior sides to the left and their dorsal sides up.

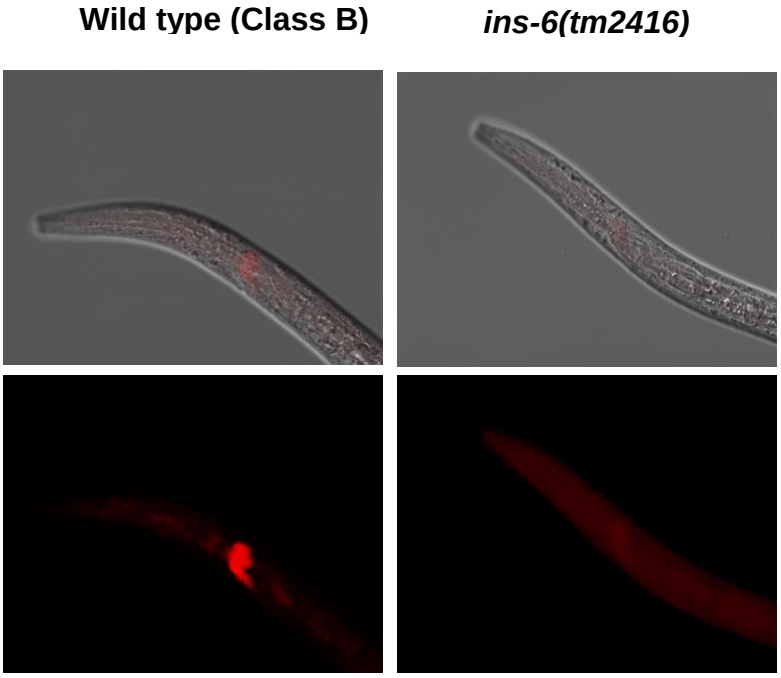

Figure 4.2 – *ins-6* null mutant dauers show significantly less or no *ins-6* mRNA in the nerve ring compared to wild-type dauers.
The left panels show a wild-type class B dauer with high levels of *ins-6* mRNA in the nerve ring. The right panels show a representative of at least twenty-two *ins-6* deletion mutant dauers that have been assayed, where there is no *ins-6* in the ASJ cell body and a very low (background) amount of *ins-6* mRNA in the nerve ring. The top panels show the DIC images of the animals and the bottom panels show the corresponding fluorescent images. Animals are oriented with anterior sides to the left and their ventral sides down.

4.2 – Different kinesins have different effects on *ins-6* mRNA subcellular localization and mRNA levels

To determine which kinesins and dyneins in *C. elegans* to analyze, the *C. elegans* genome was mined for genes that show homologies to known sequences of either kinesin or dynein proteins (in collaboration with Rashmi Chandra and Deniz Sifoglu). This led to the identification of 41 kinesins and 40 dyneins in *C. elegans*. By looking through published expression patterns (www.wormbase.org), we narrowed the list to those that only had neuronal expression. This list was further filtered to exclude those without any known mutations or those with lethal or sterile mutations (www.wormbase.org). Therefore, the final list only consists of those with available mutations that are homozygous viable and fertile [Figure 4.3]

(www.wormbase.org). For my thesis, I focused on three kinesins, *klp-4*, *klp-6* and *unc-104*, to screen for altered *ins-6* subcellular localization and expression in five-day-old dauers [Figure 4.3]. These kinesins are members of the kinesin-3/UNC-104 family, which are able to bind directly to vesicles (Klopfenstein et al., 2002), some of which can carry neuropeptides (Barkus, 2008). Additionally, they are able to carry synaptic vesicle components in the axon (Otsuka et al, 1991).

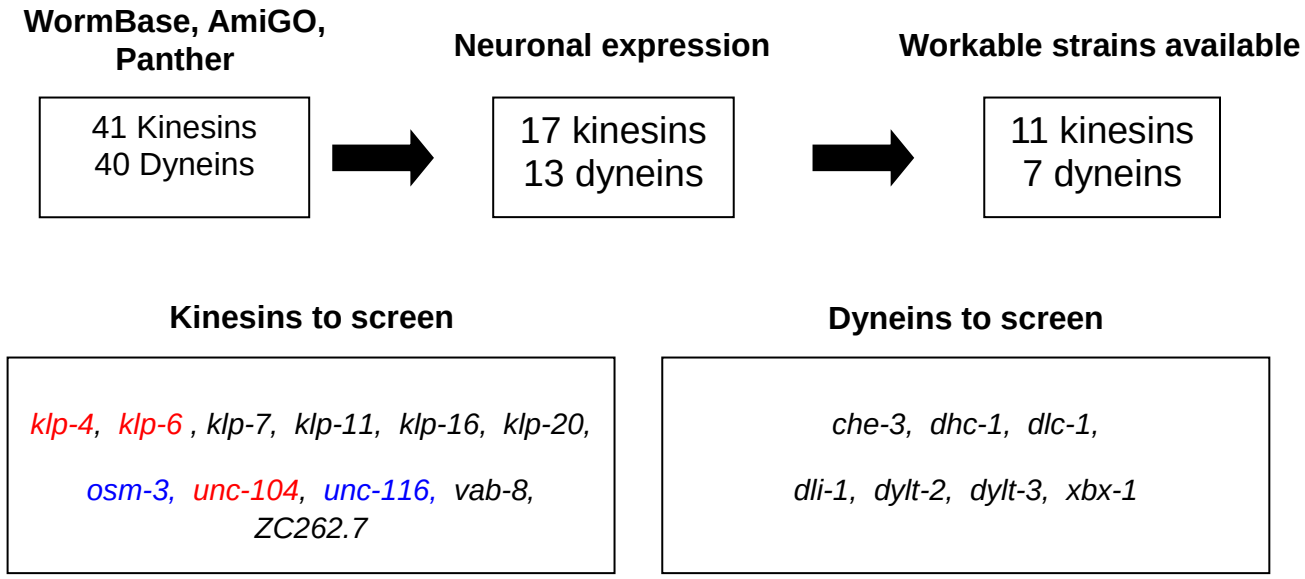

Figure 4.3 – Schematic diagram to show the selection of the candidate kinesins and dyneins to be studied.
The *C. elegans* genome was mined to look for kinesin and dynein genes. Those identified were filtered to include only those with neuronal expression. Of these neuronal kinesins and dyneins, we narrowed the list further to those with available mutations that are homozygous viable and fertile (workable strains). Those in red have been screened. Those in blue are currently in progress.

After screening the candidate kinesins, I expect the following possible outcomes: (1) the candidate kinesin affects the trafficking of *ins-6* mRNA to the axons from the cell body or vice versa; (2) the kinesin has no effect on *ins-6* mRNA trafficking, but may affect *ins-6* mRNA levels; (3) the kinesin has an effect on both *ins-6* mRNA trafficking and mRNA levels; and (4) the

kinesin has no effect on both processes. If the kinesin is trafficking the *ins-6* mRNA to the axons, I would expect that loss of function of that particular kinesin would lead to an enhancement of class A dauers, whereas the loss of a kinesin that traffics *ins-6* mRNA to the soma should lead to an enhancement of class B dauers. If kinesins are increasing or decreasing the total *ins-6* mRNA levels in the different dauer classes (outcomes 2 and 3 above), these kinesins may do so indirectly by trafficking direct regulators of *ins-6* mRNA transcription and/or stability.

First, I analyzed the subcellular localization of *ins-6* mRNA in *klp-4(ok3537)* deletion mutant dauers and tested whether these mutants had altered distribution of dauers between the two classes. Compared to wild type, the *klp-4* deletion mutants did not show altered distribution of dauers between class A and class B [Table 4.1, $p = 0.6675$]. However, they did show higher *ins-6* mRNA levels based on two independent trials [Figure 4.4] (my own experiment and R. Chandra's trial experiment). This suggests that *klp-4* likely encodes a kinesin that traffics a negative regulator of *ins-6* mRNA transcription and/or stability, but does not traffic *ins-6* mRNA itself.

Next, I analyzed *klp-6(sy511)* mutant dauers, where the *sy511* mutation introduces a premature stop into the protein, which leads to a defect in the cargo-binding ability of the protein (Peden and Barr, 2005). While my preliminary data suggest that *klp-6(sy511)* dauers did not show a difference in *ins-6* mRNA levels when compared to wild-type dauers, they interestingly suggest that there was altered distribution of *klp-6* dauers between classes A and B [Table 4.1, $p < 0.0001$], where class B dauers are enriched in these mutants. Since class B dauers have more *ins-6* mRNA in the nerve ring than in the ASJ cell body, this suggests that *klp-6* might be involved in the retrograde traffic of *ins-6* mRNA. Indeed, the roughly equal distribution of wild-type dauers between the two classes [Table 4.1] could suggest that *ins-6* mRNA is trafficked in both anterograde and retrograde directions, *i.e.*, to and from the axons of the nerve ring, during dauer arrest in wild type. However, *klp-6* is a homolog of the kinesin-3 family and is predicted to

	Wild type	***klp-4***	***klp-6***
Class A (High ASJ, low nerve ring)	18/32 (56%)	26/43 (60%)	6/26 (23%)
Class B (Low ASJ, high nerve ring)	14/32 (44%)	17/43 (40%)	20/26 (77%)

Table 4.1 – Differences in dauer distribution between the two classes according to the *ins-6* mRNA subcellular localization
Wild-type dauers were almost evenly distributed between class A and class B. The total number of dauers in each class is shown per strain. The percentage present in each class is shown in parentheses. *klp-4* dauers had the same class distribution as wild-type dauers, which was confirmed by a chi-square test ($p = 0.6675$, not significant). On the other hand, *klp-6(sy511*) mutant dauers exhibited a significant difference in class distribution, which was confirmed by a chi-square test ($p < 0.0001$).

traffic cargo towards the plus-end of the microtubules, *i.e.*, in an anterograde direction towards the axon (Peden and Barr, 2005). Thus, further experiments are needed to confirm *klp-6* function in trafficking *ins-6* mRNA.

The last kinesin I analyzed is *unc-104*, whose mutation *e1265* produced dauers similar to *ins-6* deletion mutants, *i.e.*, *ins-6* mRNA is not present in the ASJ cell body and is close to background levels in the nerve ring of these mutants ($n > 10$), This suggests that *unc-104* encodes a kinesin that does not necessarily traffic *ins-6* mRNA, but may traffic a positive regulator of *ins-6* mRNA transcription and/or stability.

Thus, it appears that different kinesins have different effects on *ins-6* mRNA levels and subcellular localization within sensory neurons, which also suggests that specific kinesins recognize specific cargoes in *C. elegans* neurons.

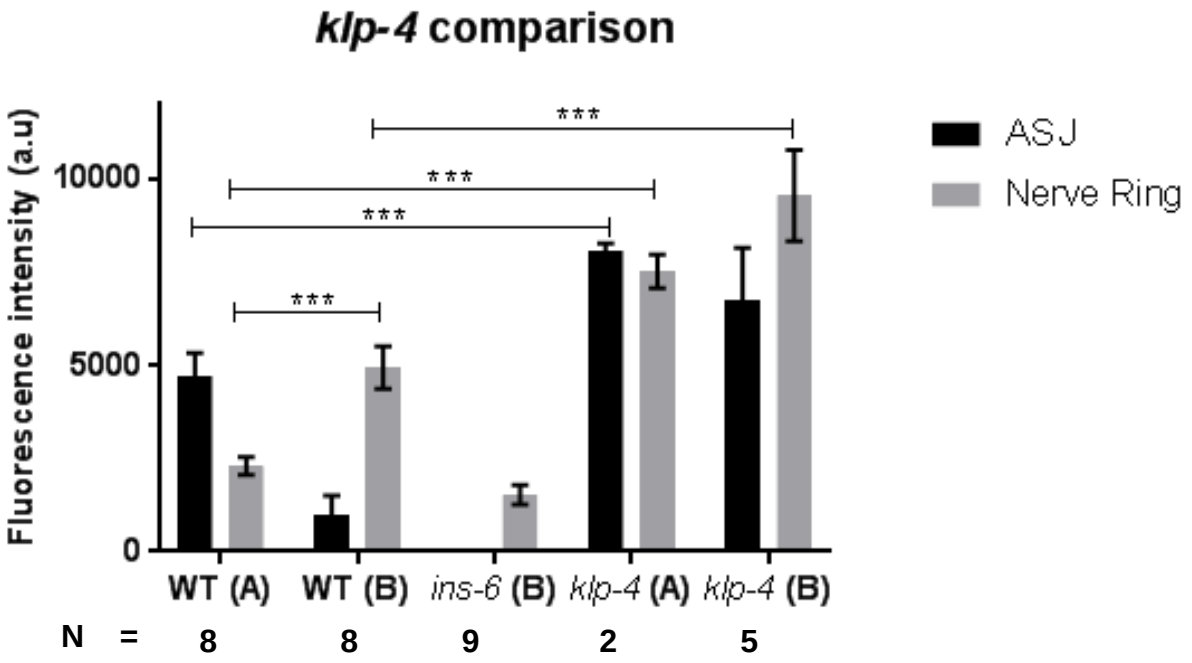

Figure 4.4 – *klp-4* may enhance *ins-6* mRNA levels in dauers.
Using images where ASJ and the nerve ring are in the same plane, *ins-6* mRNA was quantified to determine any differences in their levels. *klp-4* mutant class A and class B dauers have a significant increase in *ins-6* mRNA compared to wild-type class A and class B dauers, respectively, in both the ASJ cell body and the nerve ring. Samples were taken from the same trial. Statistics were done with unpaired t-test using Welch's correction. ***, $p < 0.0008$.

4.3 – Dauer entry phenotypes of the kinesin mutants

If the above kinesins regulate *ins-6* mRNA levels and localization within the neuron, it is possible that they also affect the dauer program, a physiological process regulated by the ILP INS-6. Thus, I measured the dauer entry phenotypes of the above kinesin mutants. Since increased relative humidity leads to higher dauer formation [Figure 3.4], I tested the kinesin mutants, using a high relative humidity of ~55% at 27^{o}C. For these experiments, I used *daf-28(tm2308)* as my positive control for dauer formation, since *ins-6* deletion mutants only produce 5% dauers at 27^{o}C (Cornils et al, 2011).

klp-4 single mutants did not display a dauer entry phenotype. Just like wild type (n = 100/trial, 2 trials), *klp-4* mutants (n ≥ 100/trial; 2 trials) formed little or no dauers at 27^{o}C ($p = 0.1061$, chi-square test). However, *unc-104* and *klp-6* did exhibit arrest phenotypes in a

separate trial. *unc-104* worms showed both high embryonic lethality and high L1 arrest [Figure 4.5]. The L1 arrest phenotype was so strong that by 42 hours, these worms did not progress past the L1 stage [Figure 4.5]. In contrast, *klp-6* mutant worms had significantly higher dauer formation compared to wild type: wild type had no animals entering the dauer program, whereas *klp-6* had 24.43% of the population in dauer arrest at 42 hours [Figure 4.5].

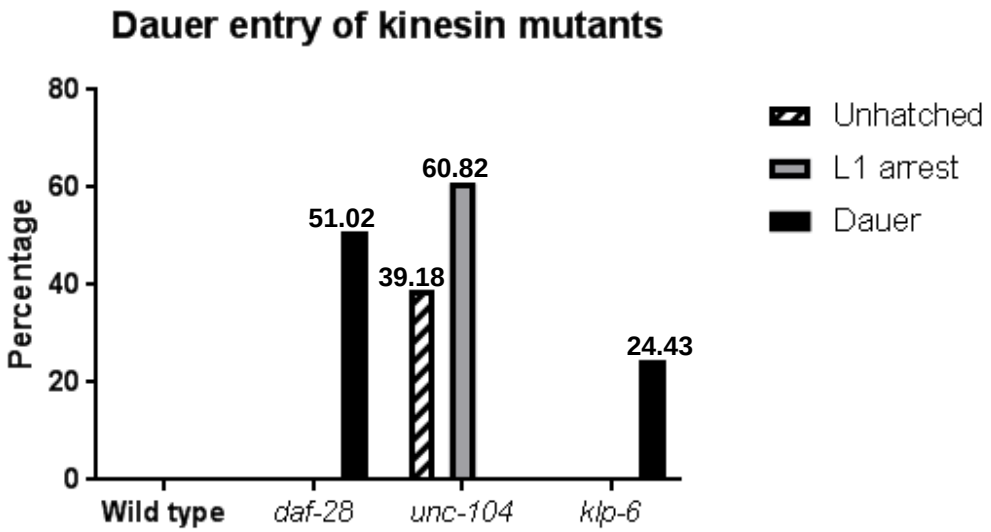

Figure 4.5 – Dauer entry phenotypes of the kinesin mutants under high humidity conditions.

At a relative humidity of 50-60%, 51.02% of the *daf-28(tm2308)* mutants, the positive control, enter dauer arrest (black bar), matching the trends observed in Basel and London ($p < 0.0001$, chi-square test, Yates correction). *klp-6* worms also exhibit a dauer entry phenotype, with 24.43% of the population forming dauers ($p < 0.0001$). In contrast, *unc-104* mutants remain arrested at the embryonic and L1 stages, which were not observed in wild type ($p < 0.0001$).

Together my data showed that the kinesins that affect *ins-6* mRNA levels and localization also had different effects on the dauer program. At present, it is hard to see a correlation between the effects of the individual kinesins on *ins-6* mRNA and entry into dauer arrest. For example, loss of *ins-6* mRNA in *unc-104* mutants did not lead to dauer arrest, but embryonic and L1 arrest, phenotypes that are atypical of *ins-6* single mutants (Cornils et al., 2011). This suggests that *unc-104* could be regulating the function of other genes that regulate arrest at earlier developmental stages. At the same time, the *klp-4* mutation alone also had little or no

effect on dauer entry. However, the *klp-4* mutation does increase *ins-6* mRNA levels [Figure 4.4], although this was observed in ASJ, and not in ASI, the dauer-inhibiting neuron (Bargmann and Horvitz, 1991). Because wild-type INS-6 does inhibit dauer entry (Cornils et al., 2011), it remains a possibility that the *klp-4* mutation will also suppress dauer entry, which may be observed only in combination with other dauer-inducing mutations. Finally, of the three kinesins, only *klp-6* exhibited a significant dauer arrest phenotype. It remains to be tested whether the enrichment of *ins-6* mRNA in the nerve ring of *klp-6* mutants is required for dauer arrest.

5. DISCUSSION

ins-6 is an important node in the insulin-like peptide (ILP) network that regulates *C. elegans* survival. It relays environmental information between ILPs to ensure reproductive growth and inhibit dauer arrest. However, *ins-6* function in regulating the switches between these two developmental programs depends on its activity in specific sensory neurons. *ins-6* acts from the ASI neuron to inhibit dauer entry and acts from the ASJ neuron to promote dauer exit (Cornils et al, 2011). Interestingly, *ins-6* mRNA also has specific subcellular localization during dauer arrest, which is lost upon exit from the dauer stage, *i.e.*, *ins-6* mRNA gets trafficked to the distal axons in dauers, but not in non-dauers or post-dauers (R. Chandra, personal communication). Together these suggest that *ins-6* expression and subcellular localization have to be regulated under different conditions. Since *ins-6* serves as a major relay within the ILP network, the regulation of *ins-6* mRNA levels and subcellular localization would also presumably regulate the state of the network, thus ensuring optimal survival of the animal in response to environmental fluctuations. My thesis focused on studying how *ins-6* expression and subcellular localization could be regulated during dauer arrest under harsh environments.

5.1 – EMS mutants likely regulate *ins-6* expression independent of the INS-6 functions in the dauer program

To study the transcriptional regulators of *ins-6*, my collaborators, R. Chandra and Z. Husain, and I conducted a forward genetic mutagenesis screen. We isolated three different classes of mutants that had varying effects on the dauer-specific expression of *ins-6*, as well as on the dauer program. For example, the class I mutants, *jx27* and *jx29*, have *ins-6* expressed in both ASI and ASJ during dauer arrest, an expression pattern that would have predicted an effect on dauer entry, but not on dauer exit. However, we find that neither mutant appears to have an effect on dauer entry [Figure 3.3], whereas *jx29* does show a delay in dauer exit, despite its wild-type *ins-6* expression in the dauer-promoting neuron ASJ [Table 3.1]. This suggests that

the targets of both mutants would be different, where the mutants regulate *ins-6* independent of the switches into and out of the dauer state.

Our screen was specific for aberrant *ins-6* expression in dauers, but normal *ins-6* expression in non-dauers (see Chapter 2.4 on chemical mutagenesis). Thus, the lack of effect of class II mutants, *jx22* and *jx24*, on *ins-6* expression in ASI, a dauer-inhibiting neuron, would have also predicted the absence of a dauer entry phenotype. Yet, *jx24* still exhibits increased dauer entry at 27^{o}C [Figure 3.3]. Moreover, this class of mutants had lower *ins-6* expression in ASJ, and only *jx24* has a delayed dauer exit phenotype, whereas *jx22* does not.

The mutations we isolated may regulate other ILPs besides *ins-6*, *e.g.*, the downstream target ILPs of INS-6, which could explain the dauer exit phenotype of *jx29* in spite of its wild-type ASJ expression of *ins-6*. These mutations may also regulate other ILPs that would compensate for the *ins-6* expression phenotype. This means that the different mutations from our screen could regulate distinct subsets of ILPs and modulate different ILP network activities. Indeed, some of the mutants could even be ILPs that we have previously identified are inhibitors, compensators or targets of *ins-6* (Fernandes de Abreu et al., 2014). Ultimately, the identification and genetic epistasis analyses among these mutations could delineate a signaling pathway that coordinates diverse physiological outputs.

5.2 – Kinesins regulate *ins-6* mRNA levels and subcellular localization

To elucidate the mechanism behind *ins-6* mRNA trafficking, we looked at mutants of three different kinesins, *klp-4*, *klp-6* and *unc-104*. Interestingly, we find that these kinesins have different effects on *ins-6* mRNA levels and localization, which would be consistent with the idea that these kinesins carry different cargoes within the *C. elegans* neurons.

5.2.1 – *klp-4 and unc-104* only affect *ins-6* mRNA levels

Interestingly, we found that two of these kinesins only affected *ins-6* mRNA levels. One of these kinesins is KLP-4, which has been classified as a member of the kinesin-3 family and

has been shown to regulate the anterograde trafficking of glutamate receptors in the *C. elegans* ventral nerve cord (Monteiro et al., 2012). The *klp-4* mutation is a deletion of about 600 bp that removes domain sequences downstream of the motor domain [Figure 5.1]. While *klp-4* mutants do not have an effect on the trafficking of *ins-6* mRNA to the distal axons [Table 4.1], they show increased *ins-6* mRNA levels [Figure 4.4, Table 5.1]. This suggests that the wild-type function of *klp-4* is either to inhibit *ins-6* transcription or *ins-6* mRNA stability. Thus, instead of trafficking *ins-6* mRNA itself, wild-type KLP-4 might carry cargo(es) that negatively regulate *ins-6* mRNA transcription and/or stability.

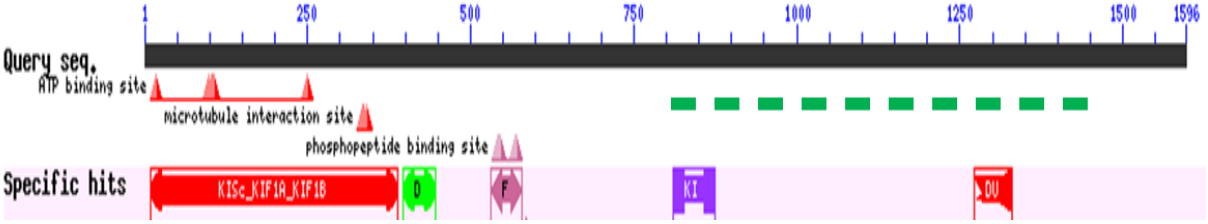

Figure 5.1 – The proposed structure of KLP-4.
The conceptual translation sequence of KLP-4 (www.wormbase.org) predicted the following protein domains: the motor domain at the N terminus (KISc/KIF1A/KIF1B, red); a forkhead associated domain that contains a nuclear signaling domain (F, magenta); a second KIF1B domain (KI, purple); and two domains of unknown function (D, green, and DU, red). The *klp-4* mutation is a deletion of approximately 600 bp, which is indicated as a green dashed line within the protein.

The other kinesin that affects *ins-6* mRNA levels is UNC-104. *unc-104* mutant dauers show little or no *ins-6* mRNA, at levels similar to that of *ins-6* null mutants [Table 5.1]. This suggests that its wild-type function is to regulate *ins-6* by either promoting *ins-6* transcription or mRNA stability [Table 5.1]. UNC-104 is predicted to be a kinesin heavy chain (Otsuka et al., 1991), and it also belongs to the kinesin-3 family (Zhou et al., 2001). The conceptual translation of the *unc-104* mutant sequence (www.wormbase.org) reveals that the wild-type aspartic acid (D) at position 1509 was substituted with an asparagine (N) [Figure 5.2]. This missense mutation is in the middle of a pleckstrin homology domain common to KIF1A and could alter its cargo-binding

activity (Klopfenstein and Vale, 2004). Thus, at least one of the cargoes trafficked by wild-type UNC-104 is likely a positive regulator of *ins-6* mRNA.

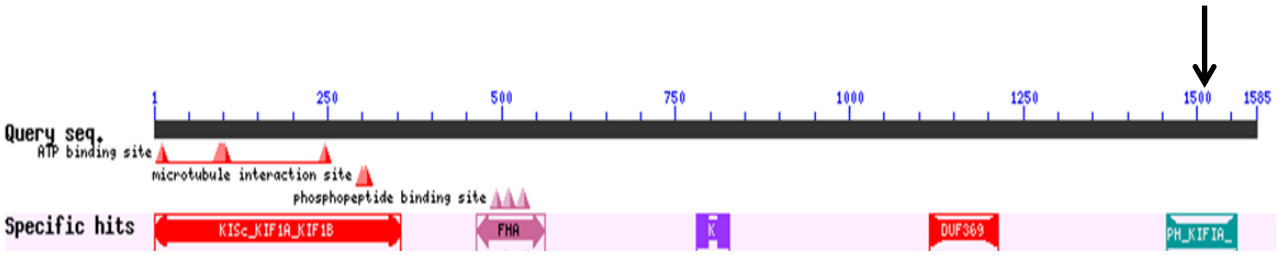

Figure 5.2 – The proposed structure of UNC-104.
The conceptual translation sequence of UNC-104 (www.wormbase.org) predicted the following protein domains: the motor domain at the N terminus (KISc/KIF1A/KIF1B, red); a forkhead associated domain that contains a nuclear signaling domain (FHA, magenta); a second KIF1 domain (K, purple); a KIF1A pleckstrin homology domain (PH_KIF1A, green); and a domain of unknown function (DUF369, red). The *unc-104* mutation studied, *e1265*, changes the wild-type aspartic acid to asparagine at residue 1509 (arrow) in the middle of the KIF1A domain (green).

5.2.2 – *klp-6* regulates *ins-6* subcellular localization

Of the three kinesins we studied, only *klp-6* appears to traffic *ins-6* mRNA within the ASJ neuron. The *klp-6* mutation introduces a stop codon at residue 709 [Figure 5.3], causing a defect in its cargo-binding activity (Peden and Barr, 2005). *klp-6* mutants have more class B dauers than class A dauers, which means a higher population of *klp-6* mutant animals have higher levels of *ins-6* mRNA localized to the nerve ring, in contrast to wild type [Tables 4.1 and 5.1]. This would suggest that wild-type KLP-6 is involved in the retrograde trafficking of *ins-6* mRNA to the ASJ cell body, Yet, the KLP-6 protein is a member of the UNC-104/kinesin-3 family and has been predicted to function in anterograde trafficking (Peden and Barr, 2005). Interestingly, however, UNC-104 has been found to move not only in an anterograde manner, but also in a retrograde manner in both *C. elegans* (Zhou et al, 2001) and *Drosophila* neurons (Barkus et al., 2008).

In *C. elegans,* GFP-tagged UNC-104 moved retrogradely approximately 10% of the time (Zhou et al, 2001). Since both KLP-6 and UNC-104 are proposed to move towards the plus ends of the microtubules, the observed retrograde movement of UNC-104, as well as possibly

of KLP-6, could mean that not all microtubules within the *C. elegans* axons have their plus ends pointed outward. Indeed, Goodwin et al (2012) showed that approximately 4% of the axonal microtubules of *C. elegans* motor neurons have their minus ends pointed outward, which could explain the retrograde movement of both UNC-104 and KLP-6. On the other hand, the UNC-104/Kif1-related kinesin-3 motors have been found to be required for dynein-mediated retrograde transport in *Drosophila* (Barkus et al., 2008). Thus, KLP-6 might also be involved in trafficking dynein motors to the plus ends of the microtubules in *C. elegans* ASJ axons or that KLP-6 activates dynein motors.

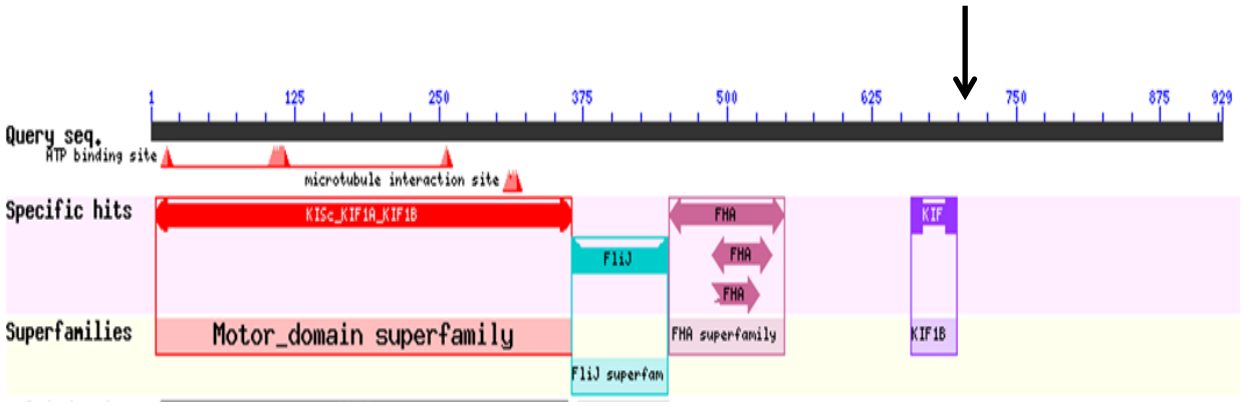

Figure 5.3 – The proposed structure of KLP-6.
The conceptual translation sequence of KLP-6 (www.wormbase.org) predicted the following protein domains: the motor domain family (red); a flagellar protein domain (light blue); the forkhead-associated domain (magenta); and the KIF1B domain (purple), which is involved in cargo-binding. The nonsense mutation at amino acid 709 is indicated by an arrow.

So far, we have found three different kinesins with distinct effects on *ins-6*, which suggests that the state of the ILP network will also depend on different combinations of kinesin activities. Indeed, some of these kinesins may traffic other ILPs that have already been shown to regulate *ins-6* mRNA levels (Fernandes de Abreu et al., 2014).

Kinesin mutant	Type of mutation	Effect on *ins-6* mRNA in dauers [Ch. 4; Figure 4.4]	Class distribution (Class A : Class B ratio) [Ch. 4; Table 4.1]	Developmental arrest phenotype [Ch. 4; Figure 4.5]
unc-104	Substitution in a coding exon (G→A). Leads to a missense mutation.	Decreases *ins-6* mRNA to levels of *ins-6* null mutants	Same as *ins-6* null mutants	Strong embryonic lethality and L1 arrest
klp-4	Deletion of ~600 bp.	Increases levels of *ins-6* mRNA	Same as wild type (Class A : Class B ratio of 3:2)	No phenotype
klp-6	Substitution (C→T). Nonsense mutation.	No effect compared to wild type	Enrichment for Class B in one trial (3:7)	~24 % form dauers

Table 5.1 – Summary of kinesin effects on *ins-6* mRNA levels and localization and on developmental arrest phenotypes

5.3 – Why does *ins-6* mRNA get trafficked to the distal axons during dauer arrest?

The observation that *ins-6* mRNA is trafficked to the axons during dauer arrest, but not in non-dauers or post-dauers (R. Chandra, personal communication) is quite intriguing. However, it remains unclear why such trafficking occurs when the animal is developmentally arrested. Dauer arrest is an animal's response to stressful environmental conditions. Thus, it is possible that ins-6 mRNA trafficking to the axons is a stress-response mechanism, which is accompanied by altered axon-to-axon communication and will require fast, local translation in response to changes within the axoplasmic environment.

REFERENCES

Allen, E.N., Ren, J., Zhang, Y., and Alcedo, J. (2015). Sensory systems: their impact on C. elegans survival. Neuroscience 296, 15-25.

Stephen F. Altschul, Thomas L. Madden, Alejandro A. Schäffer, Jinghui Zhang, Zheng Zhang, Webb Miller, and David J. Lipman (1997), "Gapped BLAST and PSI-BLAST: a new generation of protein database search programs", Nucleic Acids Res. 25:3389-3402.

Anderson, P. (1995). Mutagenesis. Methods Cell Biol 48, 31-58

Apfeld, J., and Kenyon, C. (1998). Cell nonautonomy of C. elegans daf-2 function in the regulation of diapause and life span. Cell 95, 199-210.

Bargmann, C.I., Hartwieg, E., and Horvitz, H.R. (1993). Odorant-selective genes and neurons mediate olfaction in C. elegans. Cell 74, 515-527.

Bargmann, C.I., and Horvitz, H.R. (1991a). Chemosensory neurons with overlapping functions direct chemotaxis to multiple chemicals in C. elegans. Neuron 7, 729-742.

Bargmann, C.I., and Horvitz, H.R. (1991b). Control of larval development by chemosensory neurons in Caenorhabditis elegans. Science 251, 1243-1246.

Barkus, R.V., Klyachko, O., Horiuchi, D., Dickson, B.J., and Saxton, W.M. (2008). Identification of an axonal kinesin-3 motor for fast anterograde vesicle transport that facilitates retrograde transport of neuropeptides. Mol Biol Cell 19, 274-283.

Brenner, S. (1974). The genetics of Caenorhabditis elegans. Genetics 77, 71-94.

Brogiolo, W., Stocker, H., Ikeya, T., Rintelen, F., Fernandez, R., and Hafen, E. (2001). An evolutionarily conserved function of the Drosophila insulin receptor and insulin-like peptides in growth control. Curr Biol 11, 213-221.

Bucher, E. A., and Seydoux, G. C. (1994). Gastrulation in the nematode Caenorhabditis elegans. Seminars in Developmental Biology, 5, 121-130.

Butcher, R.A., Fujita, M., Schroeder, F.C., and Clardy, J. (2007). Small-molecule pheromones that control dauer development in Caenorhabditis elegans. Nat Chem Biol 3, 420-422.

Byerly, L., Cassada, R.C., and Russell, R.L. (1976). The life cycle of the nematode Caenorhabditis elegans. I. Wild-type growth and reproduction. Dev Biol 51, 23-33.

Cassada, R.C., and Russell, R.L. (1975). The dauerlarva, a post-embryonic developmental variant of the nematode Caenorhabditis elegans. Dev Biol 46, 326-342.

Chen, Z., Hendricks, M., Cornils, A., Maier, W., Alcedo, J., and Zhang, Y. (2013). Two insulin-like peptides antagonistically regulate aversive olfactory learning in C. elegans. Neuron 77, 572-585.

Cornils, A., Gloeck, M., Chen, Z., Zhang, Y., and Alcedo, J. (2011). Specific insulin-like peptides encode sensory information to regulate distinct developmental processes. Development 138, 1183-1193.

Encalada, S.E., Szpankowski, L., Xia, C.H., and Goldstein, L.S. (2011). Stable kinesin and dynein assemblies drive the axonal transport of mammalian prion protein vesicles. Cell 144, 551-565.

Ewbank. J.J. (2006). Signaling in the immune response. WormBook, 1-12.

Fernandes de Abreu, D.A., Caballero, A., Fardel, P., Stroustrup, N., Chen, Z., Lee, K., Keyes, W.D., Nash, Z.M., Lopez-Moyado, I.F., Vaggi, F., et al. (2014). An insulin-to-insulin regulatory network orchestrates phenotypic specificity in development and physiology. PLoS Genet 10, e1004225.

Gems, D., Sutton, A.J., Sundermeyer, M.L., Albert, P.S., King, K.V., Edgley, M.L., Larsen, P.L., and Riddle, D.L. (1998). Two pleiotropic classes of daf-2 mutation affect larval arrest, adult behavior, reproduction and longevity in Caenorhabditis elegans. Genetics 150, 129-155.

Golden, J.W., and Riddle, D.L. (1982). A pheromone influences larval development in the nematode Caenorhabditis elegans. Science 218, 578-580.

Golden, J.W., and Riddle, D.L. (1984). The Caenorhabditis elegans dauer larva: developmental effects of pheromone, food, and temperature. Dev Biol 102, 368-378.

Goodwin, P.R., Sasaki, J.M., and Juo, P. (2012). Cyclin-dependent kinase 5 regulates the polarized trafficking of neuropeptide-containing dense-core vesicles in Caenorhabditis elegans motor neurons. J Neurosci 32, 8158-8172.

Grzegorz M. Boratyn, Alejandro A. Schaffer, Richa Agarwala, Stephen F. Altschul, David J. Lipman and Thomas L. Madden (2012) "Domain enhanced lookup time accelerated BLAST", Biology Direct 7:12.

Hertweck, M., Gobel, C., and Baumeister, R. (2004). C. elegans SGK-1 is the critical component in the Akt/PKB kinase complex to control stress response and life span. Dev Cell 6, 577-588.

Hirsh, D., and Vanderslice, R. (1976). Temperature-sensitive developmental mutants of Caenorhabditis elegans. Dev Biol 49, 220-235.

Jeong, P.Y., Jung, M., Yim, Y.H., Kim, H., Park, M., Hong, E., Lee, W., Kim, Y.H., Kim, K., and Paik, Y.K. (2005). Chemical structure and biological activity of the Caenorhabditis elegans dauer-inducing pheromone. Nature 433, 541-545.

Ji, N., and van Oudenaarden, A. (2012). Single molecule fluorescent in situ hybridization (smFISH) of C. elegans worms and embryos. WormBook, 1-16.

Kenyon, C., Chang, J., Gensch, E., Rudner, A., and Tabtiang, R. (1993). A C. elegans mutant that lives twice as long as wild type. Nature 366, 461-464.

Kim, K., Sato, K., Shibuya, M., Zeiger, D.M., Butcher, R.A., Ragains, J.R., Clardy, J., Touhara, K., and Sengupta, P. (2009). Two chemoreceptors mediate developmental effects of dauer pheromone in C. elegans. Science 326, 994-998.

Kimble, J., and Hirsh, D. (1979). The postembryonic cell lineages of the hermaphrodite and male gonads in Caenorhabditis elegans. Dev Biol 70, 396-417.

Kimura, K.D., Tissenbaum, H.A., Liu, Y., and Ruvkun, G. (1997). daf-2, an insulin receptor-like gene that regulates longevity and diapause in Caenorhabditis elegans. Science 277, 942-946.

Klopfenstein, D.R., Tomishige, M., Stuurman, N., and Vale, R.D. (2002). Role of phosphatidylinositol(4,5)bisphosphate organization in membrane transport by the Unc104 kinesin motor. Cell 109, 347-358.

Klopfenstein, D.R., and Vale, R.D. (2004). The lipid binding pleckstrin homology domain in UNC-104 kinesin is necessary for synaptic vesicle transport in Caenorhabditis elegans. Mol Biol Cell 15, 3729-3739.

Kodama, E., Kuhara, A., Mohri-Shiomi, A., Kimura, K.D., Okumura, M., Tomioka, M., Iino, Y., and Mori, I. (2006). Insulin-like signaling and the neural circuit for integrative behavior in C. elegans. Genes Dev 20, 2955-2960.

Larsen, P.L., Albert, P.S., and Riddle, D.L. (1995). Genes that regulate both development and longevity in Caenorhabditis elegans. Genetics 139, 1567-1583.

Lee, R.Y., Hench, J., and Ruvkun, G. (2001). Regulation of C. elegans DAF-16 and its human ortholog FKHRL1 by the daf-2 insulin-like signaling pathway. Curr Biol 11, 1950-1957.

Li, W., Kennedy, S.G., and Ruvkun, G. (2003). daf-28 encodes a C. elegans insulin superfamily member that is regulated by environmental cues and acts in the DAF-2 signaling pathway. Genes Dev 17, 844-858.

Libina, N., Berman, J.R., and Kenyon, C. (2003). Tissue-specific activities of C. elegans DAF-16 in the regulation of lifespan. Cell 115, 489-502.

Lin, K., Dorman, J.B., Rodan, A., and Kenyon, C. (1997). daf-16: An HNF-3/forkhead family member that can function to double the life-span of Caenorhabditis elegans. Science 278, 1319-1322.

Lin, K., Hsin, H., Libina, N., and Kenyon, C. (2001). Regulation of the Caenorhabditis elegans longevity protein DAF-16 by insulin/IGF-1 and germline signaling. Nat Genet 28, 139-145.

Ludewig, A.H., Kober-Eisermann, C., Weitzel, C., Bethke, A., Neubert, K., Gerisch, B., Hutter, H., and Antebi, A. (2004). A novel nuclear receptor/coregulator complex controls C. elegans lipid metabolism, larval development, and aging. Genes Dev 18, 2120-2133.

Maday, S., Twelvetrees, A.E., Moughamian, A.J., and Holzbaur, E.L. (2014). Axonal transport: cargo-specific mechanisms of motility and regulation. Neuron 84, 292-309.

Maier, W., and Neagu, A. (2011). snPCR for reliable one-step genotyping of single nucleotide differences. WormBook.

Malone, E.A., and Thomas, J.H. (1994). A screen for nonconditional dauer-constitutive mutations in Caenorhabditis elegans. Genetics 136, 879-886.

Monteiro, M.I., Ahlawat, S., Kowalski, J.R., Malkin, E., Koushika, S.P., and Juo, P. (2012). The kinesin-3 family motor KLP-4 regulates anterograde trafficking of GLR-1 glutamate receptors in the ventral nerve cord of Caenorhabditis elegans. Mol Biol Cell 23, 3647-3662.

Morris, J.Z., Tissenbaum, H.A., and Ruvkun, G. (1996). A phosphatidylinositol-3-OH kinase family member regulating longevity and diapause in Caenorhabditis elegans. Nature 382, 536-539.

Nef, S., and Parada, L.F. (2000). Hormones in male sexual development. Genes Dev 14, 3075-3086.

Nika, L., Gibson, T., Konkus, R., and Karp, X. (2016). Fluorescent Beads Are A Versatile Tool for Staging Caenorhabditis elegans in Different Life Histories. G3 (Bethesda) 6, 1923-1933.

Ogg, S., Paradis, S., Gottlieb, S., Patterson, G.I., Lee, L., Tissenbaum, H.A., and Ruvkun, G. (1997). The Fork head transcription factor DAF-16 transduces insulin-like metabolic and longevity signals in C. elegans. Nature 389, 994-999.

Otsuka, A.J., Jeyaprakash, A., Garcia-Anoveros, J., Tang, L.Z., Fisk, G., Hartshorne, T., Franco, R., and Born, T. (1991). The C. elegans unc-104 gene encodes a putative kinesin heavy chain-like protein. Neuron 6, 113-122.

Paradis, S., Ailion, M., Toker, A., Thomas, J.H., and Ruvkun, G. (1999). A PDK1 homolog is necessary and sufficient to transduce AGE-1 PI3 kinase signals that regulate diapause in Caenorhabditis elegans. Genes Dev 13, 1438-1452.

Paradis, S., and Ruvkun, G. (1998). Caenorhabditis elegans Akt/PKB transduces insulin receptor-like signals from AGE-1 PI3 kinase to the DAF-16 transcription factor. Genes Dev 12, 2488-2498.

Patel, D.S., Garza-Garcia, A., Nanji, M., McElwee, J.J., Ackerman, D., Driscoll, P.C., and Gems, D. (2008). Clustering of genetically defined allele classes in the Caenorhabditis elegans DAF-2 insulin/IGF-1 receptor. Genetics 178, 931-946.

Peden, E.M., and Barr, M.M. (2005). The KLP-6 kinesin is required for male mating behaviors and polycystin localization in Caenorhabditis elegans. Curr Biol 15, 394-404.

Pierce, S.B., Costa, M., Wisotzkey, R., Devadhar, S., Homburger, S.A., Buchman, A.R., Ferguson, K.C., Heller, J., Platt, D.M., Pasquinelli, A.A., et al. (2001). Regulation of DAF-2 receptor signaling by human insulin and ins-1, a member of the unusually large and diverse C. elegans insulin gene family. Genes Dev 15, 672-686.

Riddle, D.L., and Albert, P.S. (1997). Genetic and Environmental Regulation of Dauer Larva Development. In C elegans II, D.L. Riddle, T. Blumenthal, B.J. Meyer, and J.R. Priess, eds. (Cold Spring Harbor (NY)).

Riddle, D.L., Swanson, M.M., and Albert, P.S. (1981). Interacting genes in nematode dauer larva formation. Nature 290, 668-671.

Roostalu, J., Hentrich, C., Bieling, P., Telley, I.A., Schiebel, E., and Surrey, T. (2011). Directional switching of the kinesin Cin8 through motor coupling. Science 332, 94-99.

Rulifson, E.J., Kim, S.K., and Nusse, R. (2002). Ablation of insulin-producing neurons in flies: growth and diabetic phenotypes. Science 296, 1118-1120.

Schackwitz, W.S., Inoue, T., and Thomas, J.H. (1996). Chemosensory neurons function in parallel to mediate a pheromone response in C. elegans. Neuron 17, 719-728.

Alejandro A. Schäffer, L. Aravind, Thomas L. Madden, Sergei Shavirin, John L. Spouge, Yuri I. Wolf, Eugene V. Koonin, and Stephen F. Altschul (2001), "Improving the accuracy of PSI-BLAST protein database searches with composition-based statistics and other refinements", Nucleic Acids Res. 29:2994-3005.

Schuster, M., Kilaru, S., Fink, G., Collemare, J., Roger, Y., and Steinberg, G. (2011). Kinesin-3 and dynein cooperate in long-range retrograde endosome motility along a nonuniform microtubule array. Mol Biol Cell 22, 3645-3657.

Sherwood, O.D. (2004). Relaxin's physiological roles and other diverse actions. Endocr Rev 25, 205-234.

Tomioka, M., Adachi, T., Suzuki, H., Kunitomo, H., Schafer, W.R., and Iino, Y. (2006). The insulin/PI 3-kinase pathway regulates salt chemotaxis learning in Caenorhabditis elegans. Neuron 51, 613-625.

Vowels, J.J., and Thomas, J.H. (1992). Genetic analysis of chemosensory control of dauer formation in Caenorhabditis elegans. Genetics 130, 105-123.

Wadsworth, W.G., and Riddle, D.L. (1989). Developmental regulation of energy metabolism in Caenorhabditis elegans. Dev Biol 132, 167-173.

Ward, S., Thomson, N., White, J.G., and Brenner, S. (1975). Electron microscopical reconstruction of the anterior sensory anatomy of the nematode Caenorhabditis elegans.?2UU. J Comp Neurol 160, 313-337.

White, J.G., Southgate, E., Thomson, J.N., and Brenner, S. (1986). The structure of the nervous system of the nematode Caenorhabditis elegans. Philos Trans R Soc Lond B Biol Sci 314, 1-340.

Wolkow, C.A. (2002). Life span: getting the signal from the nervous system. Trends Neurosci 25, 212-216.

Zhou, H.M., Brust-Mascher, I., and Scholey, J.M. (2001). Direct visualization of the movement of the monomeric axonal transport motor UNC-104 along neuronal processes in living Caenorhabditis elegans. J Neurosci 21, 3749-3755.

ABSTRACT

REGULATORS OF *INS-6*, A MAJOR NODE OF THE INSULIN-LIKE PEPTIDE NETWORK FOR DEVELOPMENTAL PLASTICITY

by

LISA LI

August 2016

Advisor: Joy Alcedo

Major: Biological Sciences

Degree: Master of Science

In *C. elegans*, an insulin-like peptide (ILP) network coordinates various physiological processes, including developmental plasticity, to enhance survival under different environments. During stressful conditions, such as high temperatures, low food and high population density, first-stage larval worms enter an alternative developmental arrest program called dauer. When ideal environmental conditions are restored, worms exit from the dauer stage to go through reproductive adulthood. Different subsets of ILPs regulate the entry into versus the exit from the dauer state. For example, the ILP *ins-6* plays a minor role in inhibiting dauer entry from the ASI sensory neurons, but a more primary role in promoting dauer exit from the ASJ sensory neurons. More importantly, INS-6 also acts as a major information relay within the ILP network. Thus, identification of the regulators of *ins-6* will presumably also identify the regulators of the ILP network that ensures survival in response to changing environments. In collaboration with two other members of the lab, I performed a forward genetic screen to identify regulators of *ins-6* and to determine how these regulators affect developmental plasticity. Through this screen, we isolated five mutants.

Single molecule fluorescent *in situ* hybridization (smFISH) also revealed that endogenous *ins-6* mRNA is trafficked to the axons of ASJ neurons in dauer larvae, in contrast to well-fed, non-dauer animals. This suggests that *ins-6* is regulated not only at the transcriptional

level, but also at the post-transcriptional level, where axonal transport of *ins-6* mRNA is likely required to facilitate stress responses. Through a candidate gene approach, I investigated three candidate kinesins that could mediate this stress-dependent axonal transport of *ins-6* mRNA. My data suggest that the three kinesins, *klp-4*, *klp-6* and *unc-104* have different effects on *ins-6* mRNA, where *klp-4* and *unc-104* regulate *ins-6* mRNA levels, but not its subcellular localization. In contrast, I show that *klp-6* is involved in trafficking *ins-6* mRNA within the ASJ neurons. Thus, these kinesins, together with the mutants isolated from the forward genetic screen, presumably regulate not only *ins-6* activities, but also coordinate the different activities of the ILP network that is critical for animal survival.

AUTOBIOGRAPHICAL STATEMENT

EDUCATION

Wayne State University, Detroit, MI
Masters of Science, Biological Sciences
August 2016

Wayne State University, Detroit, MI
BS Biochemistry and Molecular Biology
December 2012
Presidential Scholar

PROFESSIONAL EXPERIENCE

GRADUATE TEACHING ASSISTANT
Wayne State University September 2013-August 2016
Anatomy and Physiology (BIO2870): Laboratory course with emphasis on anatomical systems. Utilized models and dissections of sheep and cow organs

Poster Presentation
"A stress response-dependent axonal transport of an insulin-like peptide mRNA in neurons"
Retreat of the Department of Biological Sciences, Wayne State University, October 2014

Research Assistant, Wayne State University March 2012 – May 2013
Research with Dr. Haidong Gu on the herpesvirus early gene product ICP0 and its trafficking schedule in viral-host interaction.

Poster Presentation
"Overexpression of Herpes Simplex Virus 1 VP22 accelerates nuclear to cytoplasmic translocation of ICP0"
Retreat of the Department of Biological Sciences, Wayne State University, October 2012

Student Assistant, Wayne State University Jan. 2009 – Dec. 2011
Assisted in setting up laboratory equipment for microbiology and anatomy courses
Prepared media for microbiology experiments
Supported Teaching Assistants in the classroom during lessons

EXTRACURRICULAR ACTIVITIES

Avid long distance runner

Occasionally act as a piano accompanist for local high school students in regional and state Solo/Ensemble events hosted by the Michgan School Band and Orchestra Association (MSBOA)